Riga Technical University

Faculty of Mechanical Engineering, Transports and Aeronautics

Institute of Biomedical Engineering and Nanotechnologies

Master Thesis

SIMULATION OF ELECTRON EXOEMISSION INDUCED BY MATERIAL LOADING

Author: Andrea Llop Balsebre

Supervisors: Yuri Dekhtyar

Sanda Kronberga

RTU 2020

ABSTRACT

In this thesis the connection between the elongation of the atomic bonds and the emission current in two types of materials: metals and semiconductors has been studied and identified. With this relation, two models have been constructed to simulate the emission process under strain and photostimulation. Knowing that any excitation of the electron subsystem in the solid-state exerts an influence on the emission of electrons. In total 10 metals (Na, Ca, Li, Mg, In, Zn, Pb, Sn, Fe, and Al) and 4 semiconductors (Si, Ge, GaAs and GaSb) under a tensile-strain test condition have been simulated using Matlab.

The results observe a clear tendency in metals: strain reduces free electron density and thus, the work function of the metal is decreased enabling more electrons to be emitted with photostimulation. Contrary, in semiconductors two tendencies are observed depending on the energy transitions of the materials, as the pressure potential constant can be positive or negative. Depending on this, the work function is decreased with the strain (the case of Silicon) or increased (the rest of semiconductors), this increment reduces the emission with increasing strain and pressure in semiconductors.

The results presented are self-consistent and the model can be applied successfully to account for the emission process of different metals and semiconductors. It also could be applied to different materials not studied in this thesis using appropriate parameters that need to be identified and studied with experiments.

ABSTRACTE

En aquesta tesi s'ha estudiat i identificat la connexió entre l'allargament dels enllaços atòmics i el corrent d'emissió en dos tipus de materials: metalls i semiconductors. Amb aquesta relació, s'han construït dos models per simular el procés d'emissió sota tensió i fotoestimulació. Sabent que qualsevol excitació del sistema d'electrons en l'estat sòlid exerceix una influència sobre l'emissió d'electrons. En total s'han simulat 10 metalls (Na, Ca, Li, Mg, In, Zn, Pb, Sn, Fe i Al) i 4 semiconductors (Si, Ge, GaAs i GaSb) sota les condicions simulant un assaig a tracció mitjançant Matlab.

Els resultats permeten observar una clara tendència en els metalls: la tensió redueix la densitat d'electrons lliures i, per tant, es redueix la funció de treball del metall permetent l'emissió de més electrons amb l'energia aportada per la fotoestimulació. Pel que respecta als semiconductors, s'observen dues tendències en funció de les transicions energètiques dels materials, ja que segons les característiques electròniques, la constant de pressió pot ser positiva o negativa. Depenent d'això, la funció de treball disminueix amb la deformació (com en el cas del Silici) o augmenta (en la resta de semiconductors). Així, aquest increment de la funció de treball redueix l'emissió amb l'augment de la tensió i la pressió en alguns dels semiconductors.

Els resultats presentats són consistents i el model es pot aplicar amb èxit per tenir en compte el procés d'emissió de diferents metalls i semiconductors. També es podria aplicar a diferents materials no estudiats en aquesta tesi mitjançant els paràmetres adequats que cal identificar i estudiar amb més experiments.

TABLE OF CONTENTS

LIST OF FIGURES

LIST OF TABLES

ABBREVIATIONS

Abbreviation	Meaning	Abbreviation	Meaning
Al	Aluminum	m_{rel}	Rest mass of each fermion
A	Area	Si	Silicon
k	Boltzmann constant	Na	Sodium
ε_b	Bond energy	c	Speed of light in the medium.
Ca	Calcium	σ	Stress
μ	Coefficient of the external force	T	Temperature
E_C	Conduction band energy	TSEE	Thermally-stimulated exoemission
β	Constant for the metallic model	Sn	Tin
D	Diameter	N	Total number of electrons
DSEE	Direct structural change exoemission	UV	Ultra-violet
v	Electromagnetic frequency	E_{Vac}	Vacuum level energy
χ	Electron affinity	ε_0	Vacuum permittivity
n	Electron density	E_V	Valence band energy
EPR	Electron paramagnetic resonance	V	Volume
eV	Electron-volt	r_s	Wigner-Seitz radius
τ	Endurance	ϕ or WF	Work function
E_{gap}	Energy bandgap	E	Young's modulus
ε	Engineering strain	Zn	Zinc
σ	Engineering stress		
r_e	Equilibrium distance		
EE	Exoemission		
E_F	Fermi level energy		
F	Force		
GaSb	Gallium Antimonide		
GaAs	Gallium Arsenide		
Ge	Germanium		
In	Indium		
IRS	Infrared spectroscopy		
U_0	Initial activation energy		
Fe	Iron		
K	Kelvin		
Pb	Lead		
L	Length		
L-J	Lennard-Jones potential		
Li	Lithium		
α	Madelung constant		
Mg	Magnesium		
MS	Mass spectrometry		
NMR	Nuclear magnetic resonance		
z	Number of valence electrons		
Pa	Pascals		
e	Photon energy		
PSEE	Photo-stimulated exoemission		
h	Planks constant		
x	Position		
m	Power index		
P	Pressure		
γ	Pressure coefficient of a semiconductor		

INTRODUCTION

In the mechanics of materials, the strength of a material is its ability to resist an applied load without failure or deformation. This property is one of the most relevant to characterize a material, having lots of implications in final material usage. Therefore, physics that govern this property have been studied for a long time in history and they are still a matter of interest in engineering and science of materials. Therefore, specific material tests have been developed to characterize this property for all types of materials, considering various factors that affect material's stability and chemical composition. Some of these tests have been used to prove that failure is a process that develops in time, as the kinetic conception of strength. Hence, it has been demonstrated that materials do not fail by direct mechanical rupture of interatomic bonds; they fail due to the separation of atoms.

Exoemission (EE) is the emission or ejection of an electron from the material. Some materials generate a weak electron emission when they are exposed to irradiation, tensile stress, deformation, or high temperatures since this excitation turns the objects into an unbalanced state. As material loading leads to the breakage of chemical bonds, this can be detected by the electron emission from the material using specific techniques. These techniques allow to characterize the starting of failure process and they grant the possibility to determine very slight changes in material's structure, a signal of the beginning of early destruction. Thus, experiments, where EE is studied, can substitute time-consuming endurance testing methods used until now. Furthermore, establishing models for this phenomenon can allow us to understand material properties and perform simulations of materials behavior under certain conditions. This could have practical importance aspects, for example, more centered on biomedical materials it could be used to predict the emissions of electrons, which have undesirable effects on human bodies.

Taking all of this into account having a model of electron exoemission induced by material loading could allow to predict metal and semiconductor behavior under usage conditions or anticipate its failure. To achieve this, the emission properties of these types of materials need to be assessed. Therefore, the hypothesis that failure is a process will be corroborated and the exoemission of electrons can be simulated and studied.

Therefore, the main purposes of the thesis are:

A) To identify and study the connection between the emission current of the material and elongation of the atomic bonds, due to strain
B) To build a model with the established connections and simulate the emission process under strain and photostimulation
C) To point out the use of this emission as the destruction predictor
D) To compare some existing experimental results with the simulations

This will be done in two types of materials: metals and semiconductors. Thus, to achieve this, the relations between the electron function and the elongation of the interatomic bonds need to be studied and characterized with a formula. Once the model is completed, simulation using Matlab software will enable to determine the effects of the different parameters that influence this relation.

1. LITERATURE REVIEW

1.1 Historical introduction

One of the main reasons to study materials behavior under load during history has been humans need to be able to predict the conditions in which failure is caused. Thus, the need to understand and control the fracture of solids raised theories of solid mechanics and material failure. On the one hand, solid mechanics is the study of the deformation and motion of solid materials under the action of forces. On the other hand, but related to the first one, material failure theory is the science of predicting the conditions under which solid materials fail under the action of external loads [1].

Therefore, for quantitative evaluation of the reaction of solids to mechanical influences people needed to introduce new concepts. Firstly, the strength concept: used in material science to define material's ability to resist under an applied load without failure or deformation. Secondly, to define the time until failure the concept of endurance can be used. These concepts together with elastic limit (the maximum extent to which a solid may be stretched without permanent alteration), and yield (when permanent deformation occurs), are used for quantitative evaluation of the reaction of solids to mechanical influences [2].

Initially, failure was studied within the framework of the continuous media with a purely mechanical approach to failure problems. After, when people had begun to consider solids to be structures made of atoms connected by bonding forces the theory of interatomic and intermolecular bonding forces made it possible to calculate the strengths of bonds in materials and to estimate the theoretical strength of the solids having an ideal structure. Nevertheless, experience and calculation have shown that the theoretical strength is extremely high, and it exceeds the practical strength of actual solids [3].

Though failure theory has been in development for over 200 years, no final answer has been reached to the question "why do materials fail?" To answer this question, efforts are now concentered on knowing how failure is developed in a material or component in favor to help to design against it [2]. Therefore, systematic studies have been designed and performed to understand the physics of failure in two fundamental fields: material science (design of materials with improved strength properties), and the engineering-design field (calculating and predicting the endurance of parts and structures under varying conditions of use (stress, temperatures, loading schedule, irradiation, environmental action, etc.).

1.2 The kinetic nature of the strength of solids

The main principle of the thesis is found in [3], in this article a kinetic approach to materials performance under tensile is discussed and new fundaments regarding the theory of strength are presented.

This different development of physical notions of strength was taken in the fifties to counterbalance an explanation to time and temperature dependence of the strength of solids found in numerous experiments. To answer these questions, in [3] failure is treated as an independent kinetic process that characterizes solids that vary in nature and physicochemical properties. The bases of this approach comprise numerous data from phenomenological studies

of the endurance of stressed solids and results of detailed studies of the failure process performed by modern physical methods. Thus, this approach made it possible to trace the development of failure from elementary events of breaking of overstressed interatomic bonds and appearance of nuclei of cracks, up to the formation of macro-failure cracks that bring about rupture of the object.

1.2.1 Fundamental premises of the kinetic conception of strength

In [3], it is considered that the external force acts on a system of particles in vibrational thermal motion, not on a stationary system of bound atoms, whereby the local stresses on the interatomic bonds vary. Therefore, the motion of atoms and molecules and their bounding forces are considered. This implies that in addition to the ordinary purely mechanical way of breaking interatomic bonds in which the external agent alone pulls the atoms apart when the external force reaches a limiting value equal to the strength of the interatomic bond, there is a mixed way of failure where the atoms become separated at stresses below the strength of the interatomic bonds. This implies that materials do not fail by direct mechanical rupture of interatomic bonds. When a material is stressed the interatomic distance changes and the density and energy of the bonds are altered.

Failure is treated as a unique process that develops in time, where the characters that reflect this kinetic nature is the endurance (τ) of solid objects under the stress (σ), i.e. the time that the sample exists in the stressed state from the instant of application of the load until rupture [3].

To study this behavior systematic studies of the phenomenon of time-dependence of the strength were carried out in different types of materials using direct physical methods [3]. In these experiments, the relation of endurance to the applied stress, and temperature of the test were known. As a result, these experiments led to the establishment of laws that are general for solids relating the endurance (τ) to the acting stress (σ) and the temperature (T).

The results showed that materials varied in structure and properties obey the endurance-stress relation: the endurance declines with increasing stress. This relation is linear and prevalent in all solids. Furthermore, it was observed that the time-dependence of the strength persists also in vacuum. However, the linearity of the log τ - σ relation breaks down as σ gets closer to 0 this is natural since otherwise, the object would have a finite lifetime in the absence of a load [3].

Other experiments involving interrupted loading demonstrated that the specimen was weakened after being under load for a certain time: its subsequent endurance (measured from the instant of reapplication of the same load) was reduced. This demonstrates the fact that processes of gradual accumulation of failure occur with time in a stressed object [3].

As the experiments were performed at different constant temperatures the effect of temperature on endurance under load of solids could be studied. The results showed that the log τ (σ) relation remains linear for each material, but the slopes of these lines were consistently different. The slopes of the log τ-σ lines decrease with increasing temperature and increase and approach the vertical with decreasing temperature. It is a highly essential fact that the family of linear log τ-σ relations at different temperatures is a group of straight lines that intersect at a single point. This pole was shown to occur at practically the same endurance value 10^{-13} s for all types of solids. This value is known as τ_0 and it was found by extrapolation, moreover, it is

related to the period of the intrinsic thermal vibrations of the atoms in all condensed materials, which is also close to 10^{-13} s [3].

These experiments showed that the time and temperature dependence of the strength is a phenomenon characteristic of failure of solids. Thus, the relations obtained experimentally between the endurance (τ), the stress (σ), and the temperature (T) made it possible to establish analytical relationships between these quantities. The endurance of solids proves to obey the expression [3]:

$$\ln(\tau) = \ln(\tau_0) + \frac{U(\sigma)}{kT} \quad (1)$$

Where k is the Boltzmann constant; T is the absolute temperature and $U(\sigma)$ is:

$$U(\sigma) = U_0 - \mu\sigma \quad (2)$$

Thus, they can be rewritten in the form:

$$U(\sigma) = kT \ln\left(\frac{\tau}{\tau_0}\right) \quad (3)$$

Taking into consideration these equations it was hypothesized that it is precisely the energy of the thermal fluctuation, that permits the atoms (or molecules) in the material to surmount the potential barriers that are created by the interaction of surrounding atoms with a given atom. Hence, the quantity U(σ) can be called the activation energy of the failure process. This energy depends on the applied stress and declines linearly with increasing σ [3].

The quantity U_0 (the initial activation energy) was determined by experiments to measure the endurance, where U(σ) was extrapolated to σ=0. Obtained values of U_0 found from experimental data were compared with the activation energies for thermal decomposition of interatomic bonds (the energy of sublimation in metals and the energy of thermal decomposition in polymers). Both values resulted to be remarkably close. Therefore, it was established that the energy of thermal fluctuations and the separation of atoms in solids under stress, is the essence of the failure process [3].

U_0 proves to remain constant for a given substance when its structure is changed. Nevertheless, in distinction to U_0 and τ_0, the coefficient μ is readily altered by treatment of the material. Since its physical meaning is related to the work that the external force performs in the failure of the material. Thus, the necessary energy to break the bounding atoms is a mixture of the external force and the fluctuations of the interatomic energy [3].

According to [3], the breakage of interatomic bonds is caused by the thermal fluctuations, rather than the action of the stresses. However, mechanical stress plays an extremely large role in the system of kinetic ideas as well. Applying an external load to material stresses the interatomic bonds, owing to the heterogeneity of structure of actual objects, the external load is distributed inhomogeneously over the bonds, and local overstresses arise. The activation energy of the interatomic bonds is lowered especially strongly at these sites where defects or imperfections are located, it is precisely at these sites that the processes of breakage of stressed bonds occur most intensively. Failure cracks are formed in those sites, and their development culminates in the breakage of the object into pieces.

1.2.2 Crystallographic defect

All crystalline solids can have imperfections in the regular geometrical arrangement of the atoms. These imperfections can result from deformation of the solid, rapid cooling from high temperature, or high-energy radiation striking the solid. They can be located at single points, along lines, or on whole surfaces in the solid, and, as it has been presented in the last section they have influence in materials mechanical, electrical, and optical behavior. Therefore, they need to be studied to establish their contribution to understanding material fracture [4].

1.2.2.1 Point defects

Point defects are defects that occur only at or around a single lattice point [5].

A) Vacancy defects are lattice sites that would be occupied in a perfect crystal but are vacant.
B) Interstitial defects or Frenkel defects are atoms that occupy a site in the crystal structure at which there is usually not an atom. They are generally high-energy configurations.
C) A substitutional defect can be caused by impurity: foreign atoms that replace some of the atoms making up the solid or that squeeze into the interstices; they are important in the electrical behavior of semiconductors.

1.2.2.2 Linear defects

Line defects, or dislocations, are lines along which whole rows of atoms in a solid are arranged anomalously. The resulting irregularity in spacing is most severe along a line called the line of dislocation. A dislocation can be characterized by the distance and direction of movement it causes to atoms which are defined by the Burgers vector. The number and arrangement of dislocations influence many of the properties of materials [6].

Line defects can weaken or strengthen solids. There are two basic types of dislocations, edge dislocation, and screw dislocation. "Mixed" dislocations, combining aspects of both types, are also common [6].

Dislocations can move if the atoms from one of the surrounding planes break their bonds and rebond with the atoms at the terminating edge. It is the presence of dislocations and their ability to readily move (and interact) under the influence of stresses induced by external loads that leads to the characteristic malleability of metallic materials and their plastic deformation. Therefore, understanding the movement of dislocation is key to understanding why dislocations allow deformation to occur at a much lower stress than in a perfect crystal [6].

1.2.2.3 Surface defects

Surface defects may arise at the boundary between two grains, or small crystals, within a larger crystal. The rows of atoms in two different grains may run in slightly different directions, leading to a mismatch across the grain boundary. Also, it can be established that the external surface of a crystal is also a surface defect because the atoms on the surface adjust their positions to accommodate for the absence of neighboring atoms outside the surface [7].

Also, three-dimensional macroscopic or bulk defects such as pores, cracks, or inclusions can be found in crystalline materials.

1.2.3 Fracture of materials

According to [8] fracture is the separation of a body into two or more parts because of applied stress. Applied stress can be in form of tensile, compressive, shear, or torsion. The present study is restricted to uniaxial tensile stress. Materials can present two different types of fracture: ductile or fragile depending on the capacity to yield. Ductile materials can absorb more energy before the fracture occurs, contrarily fragile materials do not present plastic deformation and they cannot absorb energy.

As described in [9] fracture of materials can be accompanied by the emission of particles from the material, due to the high concentration of energy deposited into a small volume of material during crack propagation for a short time. Since defects and dangling bonds are produced during fracture process electrons can get trapped or emitted. The consequences of crack growth and dislocations could contribute to this emission of particles from the material. Even though for large band gap insulators it is doubtful that the peak localized of energy reached is sufficient to elevate the valence band electrons into the vacuum. However, the energy might be quite adequate to excite and release electrons from surface traps. Likewise, thermal stimulation of the defects produced during fracture can lead to several de-excitations and recombination which produce electron, ion, and neutral particle emission as well as photons. Therefore, it can be established that before rupture, the samples under tension suffer minor failures, these failures consist primarily of fiber breakage and produce electron emission, finally as these minor failures accumulate, the entire strand fails producing a large amount of delamination, producing the major emission. The results presented in [9] show that emission during fracture is indeed a widespread phenomenon; since it has not yet found a material that does not produce some form of fracture emission. For all materials, the emission accompanying the motion of the crack-tip appears to be most intense.

1.2.4 Study of the process of failure of materials by direct physical methods

Different experiments have been conducted by direct physical methods recently allowing to study the failure of materials on the atomic-molecular level. Hence, different techniques can be used in order to study failure process: infrared spectroscopy (IRS), electron paramagnetic resonance (EPR), mass spectrometry (MS), nuclear magnetic resonance (NMR), etc. The use of the cited methods creates great potentialities for getting direct and detailed information on the initiation and growth of failure. The disadvantage of these methods is that they have greater selectivity than with phenomenological studies because any material that is suitable for study

by one direct method can prove to be poorly suitable for study by other methods. Therefore, the problem of successful choice of objects for a complex study of failure by direct methods plays an especially important role [3].

Failure of materials at the level of elementary events can be divided into three stages:

A) Overstressed bonds in loaded materials:
As described in [3] stretching the interatomic bonds decreases the bonding energy, and consequently, reduces the vibration frequency of the bonds. The stressed material contains interatomic bonds having large overstresses as compared with the mean stress. These bonds amount to a small fraction of the total number of bonds in the material. However, their presence plays a decisive role in the failure of the material, since these bonds are precisely those first broken, and this leads to the appearance of failure nuclei in the material.
The structural inhomogeneity of most actual materials and their defect nature easily explain in principle the reasons for the inhomogeneous distribution of stresses throughout the material. In polycrystalline materials, the interaction of dislocations with grain boundaries and boundary zones between the mosaic blocks are the sites of origin of failure.

B) Decomposition of the overstressed bonds:
The primary consequence of the rupture of a chemical bond is the appearance of unsaturated valences or free radicals. Experimental data showed that chemical bonds are broken in stressed materials long before the specimens failed.
These cracks appear specifically under load (there are practically none of them before applying the load) and irreversibly (removal of the load does not heal the cracks). Thus, the formation of a submicrocrack is produced in an explosive way, initiated by the primary rupture of one of the overstressed molecules in the layer. After nuclear, submicroscopic cracks have been formed, the further development of failure can consist in the merger of these cracks and formation thereby of larger cracks. Such cracks have been found upon stressing amorphous polymers as well as rock-salt crystals and metals [3].

C) Stabilization and accumulation of the broken bonds:
Free radicals initiate various chemical processes that can acquire the nature of chain reactions. This accelerates the failure of the material.

1.3 Band Theory

1.3.1 Description

The Band Theory was developed using the knowledge gained during the quantum revolution in science. It was during 1928 when Felix Bloch applied the quantum theory to solids. Before, in 1927, Walter Heitler and Fritz London discovered bands, i.e. very closely spaced orbitals with not much difference in energy [10].

Band theory, in solid-state physics, is a theoretical model describing the states of electrons, in solid materials, that can have values of energy only within certain specific ranges. The ranges of allowed energies of electrons in a solid are called allowed bands. Certain ranges of energies between two such allowed bands are called forbidden bands (i.e., electrons within the solid may not possess these energies). The band theory accounts for many of the electrical

and thermal properties of solids and forms the basis of the technology of solid-state electronics [11].

There are many energy bands, the following are the three most important energy bands in solids [10]:

A) Valence band: This band consists of valence electrons energy. The valence band is present below the conduction band and the electrons of this band are loosely bound to the nucleus of the atom.
B) Conduction band: The energy band that consists of free electrons energy levels, is known as the conduction band. For electrons to be free, external energy must be applied such that the valence electrons get pushed to the conduction band and become free.
C) Forbidden band: The energy gap between the valence band and the conduction band is known as the forbidden band which is also known as the forbidden gap. The electrical conductivity of a solid is determined from the forbidden gap.

A variety of ranges of allowed and forbidden bands is found in pure elements, alloys, and compounds. Three distinct groups are usually described: metals, insulators, and semiconductors. In metals, forbidden bands do not occur in the energy range of the most energetic electrons. Accordingly, metals are good electrical and heat conductors. Insulators have wide forbidden energy gaps that can be crossed only by an electron having an energy of several electron volts. Because electrons cannot move freely in the presence of an applied voltage, insulators are poor conductors. Semiconductors have relatively narrow forbidden gaps, which can be crossed by an electron having an energy of roughly one electron volt, and so they are intermediate conductors.

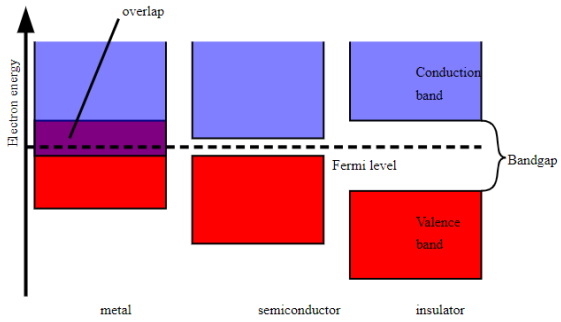

Figure 1 Representation of the energetic bands in metal, semiconductor, and insulator materials. Extracted from [12]

1.3.1.1 Conductors

Metals are materials characterized by properties such as malleability (they can be hammered into thin sheets) or ductility (can be drawn into wires). Moreover, they have high heat and electric conductivity and, if polished, they have a shiny surface. Their structure and the nature of metallic bonds explain some of these typical features. Metals are made up of positive ions tightly packed together in crystalline solids. The positive ions are surrounded by electrons, these valence electrons are free to move away from their atoms of origin. Therefore, the electrons involved become delocalized and the atomic structure of metal can effectively be visualized as a collection of atoms embedded in a cloud of relatively mobile electrons. This

explains the ability of metals to conduct heat and electricity. Also, the mechanical properties of metals, such as hardness, ability to resist repeated stressing (fatigue strength), are often attributed to the structure of the crystal structure and the defects or imperfections on it [13].

In most cases, metals have a relatively simple crystal structure distinguished by a close packing of atoms and a high degree of symmetry. Metal may be a chemical element such as iron; an alloy such as stainless steel; or a molecular compound such as polymeric sulfur nitride [14].

1.3.1.2 Dielectrics and semiconductors

A dielectric material is an electrical insulator that can be polarized by an applied electric field. Hence, it is a poor conductor of electricity, but an efficient supporter of an electrostatic field, this material can store energy. Some of the examples of solid dielectric materials are ceramics, paper, mica, glass, etc. Liquid dielectric materials examples are distilled water, etc. Gas dielectrics are nitrogen, dry air, helium, oxides of various metals, etc [15].

Dielectric materials have no free charges because all the electrons are bound and associated with the nearest atom. In isolators, the interatomic bond is ionic or strongly covalent [16].

The bandgap of dielectrics E_G is typically larger than 4 eV. *Fig. 2* shows a typical band edge diagram for a semiconducting material. Here, the energy levels E_C, E_V and E_F are the conduction band energy, the valence band energy, and the Fermi level, respectively. The activation energy of an electron from the valence band to the conduction band requires the energy of the bandgap. This type of energy can be supplied either by potential, kinetic or thermodynamic nature [17].

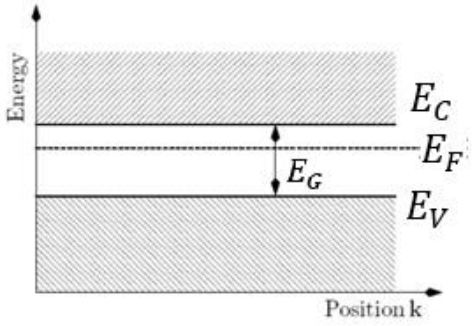

Figure 2 Idealized band diagram for a semiconducting material with the different energy levels resulting from the band structure. Adapted from [17]

Semiconductors are materials that have a conductivity between conductors (generally metals) and nonconductors or insulators (such as most ceramics). Semiconductors can be pure elements, such as silicon or germanium, or compounds such as gallium arsenide or cadmium selenide [8]. In semiconductors, the interatomic bonding is covalent and relatively weak. Thus, valence electrons are not strongly tight to the nucleus and they can be excited easily, overcoming the forbidden gap.

Further, as described in [18] dielectrics generally cannot absorb visible or near-infrared light, because the photon energy is not sufficient energy for transitions from the valence band, to the conduction band, or in fact for any kinds of transitions of carriers. Only in the ultraviolet

region, photon energies become sufficient for interband transitions. On the other hand, semiconductors because of the narrow bandgap have some electrical conductivity, since thermal excitation creates some small population of the conduction band and a corresponding population of holes in the valence band. Another consequence is that photons with moderate energy can cause interband transitions.

1.4 Exoemission

It has been proved in [19] the existence of several effects associated with the mechanical behavior of solids when a material is subjected to a constant strain rate: emission of particles (charged and/or neutral), light, or sound. The liberation or expulsion of particles; in particular electrons, from any surface of a material is called electron exoemission (EE). In this section, experimental information and mechanisms for exoemission have been described briefly, concretely, EE from metals and dielectrics.

1.4.1 History

The phenomenon of exoemission was reported by McLennan in 1902. However, it was mainly after the introduction of the Geiger tube in the 1920s that the effect was truly recognized. This phenomenon was first carefully investigated by Kramer (1950). Kramer himself found that all recently prepared metal surfaces gave off electrons and suggested that the electrons gained the required energy for coming out of metal by acquiring some of the energy released in the exothermal processes occurring on the surface [19].

1.4.2 Exoemission in Biomaterials research

Biomaterials comprise an increasingly wide variety of material types: ceramic, plastic, or polymeric materials are examples of materials that are being used, or proposed for use, as replacements for biological tissue. Such materials are now widely accepted in the medical and dental professions and implant surgery has become a reality for many thousands of people. However, as presented in [20] the consequences of the sub-microscopic reactions of such materials in the body have not been properly studied. There is often no information available on the development of surface changes on such materials or indeed their consequences in terms of cellular behavior despite it is of fundamental interest in understanding the biological response to biomaterials since there is considerable evidence that cell behavior is influenced by the surface change of solid substrata.

Accordingly, [20] exoemission phenomena could be directly applicable to understanding interfacial events brought about when a solid substrate is introduced into a liquid environment, therefore exoemission measurements could be used to predict biomaterial behavior. If the influence of the dynamic surface change characteristics of biomaterial on cell behavior can be understood then, ultimately, materials could be manufactured with specific surface change-carrier emission profiles with the aim of mimic a required biological response.

1.4.3 Main features of EE

EE occurs in various materials; the main features of this phenomena are described in [19] and they can be summarized as follows:

A) The material exhibiting EE must be excited externally to produce a perturbation in the form of a structural change. The external excitation may be in the form of cold working, irradiation by electromagnetic radiation (UV or higher frequencies), particle bombardment (α, β-rays, neutrons, protons, slow electrons, ions), exposure to gases, abrasion, mechanical deformation, etc.

B) The effect is strongly correlated with relaxation processes in the material. Which normally depends strongly on the amount and nature of the defects in the system. It is this aspect of the EE process that makes it an attractive nondestructive technique of characterizing a material for its defect contents.

C) Unlike stationary effects, such as photoemission and thermionic emission, EE is a nonstationary process.

D) The emission may be spontaneous or may require external stimulation, in addition to the external excitation. The stimulation may be in the form of increased temperature (thermally-stimulated exoemission (TSEE)) or electromagnetic radiation (photo-stimulated exoemission (PSEE)).

E) The EE effect has two components, one of which is volume dependent and the other, surface dependent. For a particular system, one or both may occur depending on the material and its surface condition as well as its surrounding gas medium. The surface effect is strongly related to the surface condition, and in a controlled EE experiment, it is often desirable to have an ultra-high vacuum (~10-10 Torr) to separate the surface effect from the volume effect. It is also desirable to have an experimental arrangement for characterizing the surface condition of the sample.

F) EE can occur continuously or in large bursts. It is usually believed that the continuous emission is related to the motion of defects in the sample, whereas the emission in bursts is related to the propagation of cracks (or micro-cracks). Thus, the nature of the EE may reveal the nature of its source.

1.4.4 Experimental arrangement

To measure EE a special experimental arrangement is necessary [19]. First, it is needed to settle an excitation unit (for example an arrangement for producing uniaxial tensile strain at a constant rate or an ultraviolet radiation unit) and a detection unit (spectrometer) attached to an ultrahigh vacuum (UHV) chamber containing the sample. Also, it should be equipped with an Auger spectrometer and a quadrupole mass analyzer for structural and chemical analysis of the surface of the sample and the identification of the chemical composition of the residual gases in the chamber. Furthermore, a facility for measuring the work function (e.g., by the Kelvin or Fowler method) is desirable.

1.4.5 Types of excitations

EE can be induced thermally (when a sufficient level of thermal energy is provided to the material), chemically, by an electrical field, when materials are exposed to electron beams with high kinetic energy or others. The main physical mechanisms inducing electron emission that will be discussed in this thesis are:

1.4.5.1 Excitations through direct structural change (DSEE)

In several materials, direct structural changes induced by external application of stress, or by generating stress internally through heat treatment can produce EE [9].

DSEE during tensile deformation and fracture was reported in the 1950s and several interesting studies followed. Electron microscopy, autoradiographic stripping, and photoemission spectroscopy showed that these signals were strongly associated with the formation of slip lines and bands on deformed surfaces [21].

Since mechanical deformation generates a high concentration of defects (vacancies and dislocations) and the relaxation of the stress is accompanied by the diffusion of vacancies towards the surface and the recovery of dislocations. These defects can rearrange themselves exothermally, and the localized release of thermal energy may be taken up by electrons. However, emission of these electrons would require a substantial lowering of the work function ϕ, which is believed to be due to high roughness on a clean metal surface [19].

The emission depends on the strain rate. The burst emission has been associated with the propagation of cracks or micro-cracks. The continuous EE is believed to arise from two components, one controlled by the diffusion of point defects (generated by strain) towards the surface, and the other controlled by the relaxation of dislocations. One may dominate over the other, or both may be present [19].

1.4.5.2 Excitation by photons (PSEE)

In the case of photo-stimulated exoemission (PSEE) light, a flow of photons striking on the material surface enables that some of the photons transfer their energy to the electrons. Considering light as a stream of photons that have an amount of energy associated (e), that is the product of electromagnetic frequency (v) of the incident light and Planks constant (h). This energy can be transferred to the electrons during the collision of photons with electrons. Electrons emitted in this manner are called photoelectrons [22].

$$e = h\,v \tag{4}$$

Therefore, if the transferred photon energy is greater than the work function of the material can cause the electrons to be pulled out from the surface, producing electron emission. The amount of photoelectric emission depends upon two factors: one is the frequency of incident light, other is the intensity of light (density of photons). Part of the acquired energy by the electrons is used to liberate the electron from its atomic binding, and the rest contributes to the electron's kinetic energy as a free particle. Because electrons in a material occupy many

different quantum states with different binding energies, and because they can sustain energy losses on their way out of the material, the emitted electrons will have a range of kinetic energies. The electrons from the highest occupied states will have the highest kinetic energy [22].

1.4.6 Mechanism and a general understanding of electron emission

Any excitation of the electron subsystem in the solid-state exerts an influence on the emission of electrons. As it has been discussed, every element can be characterized by its electronic configuration i.e. by the distribution of electrons surrounding its nucleus. In electron emission, particular interest relies upon the valence electrons (electrons in the outermost shell). This is because these are the electrons that can be easily liberated from the force of attraction. However, the energy which must be supplied differs from element to element and is regarded to be its threshold energy or work function.

1.5 Work Function

The work function (WF) of a material is defined as the minimum amount of thermodynamic work (energy) required to remove an electron from a solid to a point in the vacuum immediately outside the solid surface. The symbol for WF is ϕ [23].

Considering that the material is under photo-stimulation electrons start to be emitted from the material after a certain minimum frequency of incident light v_0 Hz. Above this frequency the kinetic energy of the emitted electrons is proportional to incident light frequency. Below, frequency v_0 or below energy hv_0 (h is Planck Constant) there will be no electron emission. This amount of energy hv_0 is known and defined as work function ϕ. Thus, the gain of the kinetic energy of an electron E_k is the difference between incident photon energy and work function of the metal or material and that can be represented as [23]:

$$E_k = hv - \phi \tag{5}$$

Where ϕ is the work function of the material and E_k is the kinetic energy gain of the electron. The equation can be rewritten as

$$E_k = hv - hv_0 \tag{6}$$

Where v_0 is threshold frequency of the material.

If the frequency of light is higher than that above-mentioned minimum frequency, the extra energy of the photon will be converted to the kinetic energy of the emitted electron. Hence, how fast the electron will be emitted from the surface of the metal depends upon the frequency of incident light. If the photon's energy is greater than the substance's work function, photoelectric emission occurs, and the electron is liberated from the surface. Otherwise, when the intensity of incident light is increased without changing its frequency the number of photons strikes on the metal surface increases, therefore more emitted electrons will be produced, despite the kinetic energy of each electron will be unchanged as the frequency of incident light is fixed [22].

This process may be corroborated by measurements of photo- and exoelectron emission. For example, PSEE can be recorded from an object irradiated with ultraviolet photons, their energy being close to the red border of the photo effect (2-5eV). In this case, according to [24] the current of electrons emitted from the solid-state (I) may be described by the relation:

$$I \approx (hv - \phi)^m \tag{7}$$

Where hv is the energy of a photon, ϕ is the photoelectric work function of the material and m is the power index. Variations of the solid-state electronic structure (for instance because of the appearance of defects, broken bonds, and so on) change ϕ, therefore, also I.

1.5.1 Methods of Measurement

The work function of solid can be determined experimentally using absolute or relative approaches [25]. Absolute methods allow one to measure the work function value directly since the electrons in the material are supplied with sufficient energy to overcome the barrier at the surface/vacuum interface and can escape the surface barrier. The work function can be obtained from the resulting electric current. Absolute methods include measurements based on thermionic emission, field emission, and the photoelectric effect. Since the energy of UV is relatively low, it can only emit valence electrons to reveal valence band structure and the magnitude of ϕ can be recorded for a condition I=0, i.e. ϕ=hv according to [24] and *Eq. (7)*.

On the other hand, relative methods employ a reference made of a material with a known work function and focus on measuring differences in electrical quantities between the studied material and the reference. This can be achieved because, when two materials are in contact, electrons of higher electrochemical potential in one material flow to the other material until the electrochemical potentials of the two metals are equal. These methods include diode methods and condenser methods (Kelvin probe) [25].

1.5.2 Work function in metals

Metallic materials consist of plenty of free electrons moving inside the metallic crystal, without leaving the surface of the metal. Free electrons cannot leave the surface of the metal due to the attractive forces of interatomic boundaries. To leave the metallic surface an electron must cross a potential barrier called surface barrier, to overcome it, the electron needs to be excited with external energy. Therefore, free electrons have kinetic energy, but this is not enough to overcome this barrier, and the extra energy required to just overcome the surface barrier is called work function, which can be different from metal to metal. Metal's work function is typically 3–5 eV [23].

$$\phi = E_{Vac} - E_F \tag{8}$$

In metals, valence bands are filled with electrons up to the Fermi energy (E_F). The energy difference between Fermi energy and vacuum level (E_{Vac}) corresponds to the work function (ϕ). In metals, work function and ionization energy are the same. The work function of a material is strongly affected by the condition of the surface. The presence of minute amounts of contamination or the occurrence of surface reactions (oxidation or similar) can change the

work function substantially. Changes of the order of 1 eV are common for metals and semiconductors, depending on the surface condition. These changes are a result of the formation of electric dipoles at the surface, which changes the energy an electron needs to leave the sample [26].

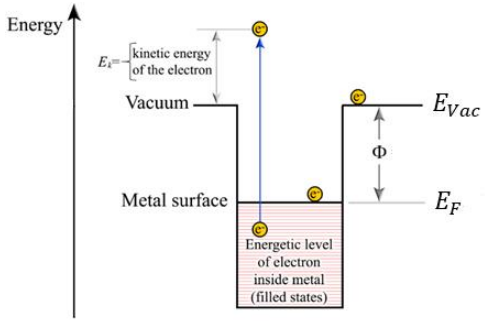

Figure 3: Schematic energy diagram of a generic metal. Extracted from: [27]

Although WF appears to mainly represent the behavior of electrons at the surface, it fundamentally characterizes the atomic interactions or the involvement of electrons in the electrostatic interaction between electrons and positively charged nuclei in a metal. Thus, WF is a fundamental property that could be used to predict and evaluate the bulk properties of materials, including mechanical behavior [28].

1.5.2.1 Influences in the electron work function of metals

It has been proved that the intrinsic mechanical behavior of materials is mostly governed by their electron behavior, which determines the atomic bond strength and configuration [8]. Considerably effort has been made to investigate the correlation between the WF and mechanical properties [29], [30], [31], [32], [33]. Therefore, experiments have been conducted to correlate the mechanical properties of materials to their electron configurations based on quantum mechanics. In the next sections, some of the influences in the work function will be discussed.

1.5.2.1.1 Yielding point and electron work function relation

The effect of deformation in the electrons and the behavior of electrons inside of the material during the tensile stress test has been the subject of studies. The Kelvin probe technique was applied to investigate the effect of tensile on WF and its physical mechanism. Taking into consideration the model presented by G. Hua and D. Li in [30], the work function of materials can be expressed as:

$$\phi = \frac{\alpha}{r_s^{3/2} E_F^{3/2}} \tag{9}$$

Where E_F is the Fermi level, α is a constant and r_s is Wigner-Seitz radius of the material [34]. Since both r_s and E_F are correlated to electron density of the materials WF can be determined by the electron density:

$$\frac{4}{3}\pi r_s^3 = \frac{1}{n} \tag{10}$$

$$E_F = \frac{h^2}{2m}(3\pi^2 n)^{2/3} \tag{11}$$

$$\Phi \propto n^{1/6} \tag{12}$$

Where m is the effective mass of an electron, h is Planck's constant, n is the electron density.

Free electron density (n) is a concept used to describe electrons' behavior in a metal. This concept is presented in a model that considers that all the electrons in the metal are like a gas that surrounds the nucleus since all the electrons are free to move from one side to the other inside the material. Therefore, this is a factor in determining its electrical conductivity [35]. Because electrons are fermions and obey the Pauli exclusion principle, at 0 K temperature the electrons fill all available energy levels up to the Fermi level. Therefore, the free electron density of a metal is related to the Fermi level and can be calculated knowing the Fermi energy of the different metals, which is tabulated [36].

Young's modulus is defined as the second-order derivative of interaction potential concerning the equilibrium distance. The interaction potential of one valence electron can be expressed as [30]:

$$\mathrm{U} = \frac{\alpha z e^2}{a} \tag{13}$$

Where α is the Madelung constant, e is the elementary charge, z is the number of valence electrons, a is the equilibrium distance between a pair of adjacent positive and negative charges. According to the definition of Young's modulus, one may obtain Young's modulus described in terms of equilibrium distance [30]:

$$E = \left.\frac{d^2U(r)}{dr^2}\right|_{r-r_0} = \frac{2\alpha z e^2}{a^3} \tag{14}$$

WF is derived:

$$\phi = \frac{e^3 m^{1/2} n^{1/6}}{16\sqrt[3]{3}\pi^{5/3} h \varepsilon_0^{3/2}} \tag{15}$$

Where n is the electron density, m is the electron mass, $\varepsilon_0$is the vacuum permittivity, h is Planck's constant.

As the electron density is inversely proportional to lattice distance [30]:

$$\mathrm{n} = \frac{z}{a^3} \tag{16}$$

WF can be expressed as:

$$\phi = \frac{e^3 m^{1/2} z^{1/6}}{16\sqrt[3]{3}\pi^{5/3} h\varepsilon_0^{3/2} a^{1/2}} \tag{17}$$

Considering the relations with Young's modulus relationship can be established as [30]:

$$E = 2\alpha z e^2 \left(\frac{16\sqrt[3]{3}\pi^{5/3} h\varepsilon_0^{3/2}}{e^3 m^{1/2} z^{1/6}}\right)^6 \phi^6 \propto \beta\phi^6 \tag{18}$$

This formula describes a six-power relationship between Young's modulus and WF ($\beta$is a constant).

Experimental results in [28] showed that tensile strain decreased WF in the elastic deformation range, while compressive strain increased WF. However, WF in the plastic deformation range always decreased with plastic strain no matter whether it was tensile or compressive since introduced dislocations associated with plastic deformation make the potential well shallower. According to this model plastic deformation involving dislocations should always decrease the WF, but the WF should increase or decrease with compressive deformation or tensile deformation, respectively, in the elastic range without dislocation involved.

1.5.2.1.2 Influences of deformation in the electron work function

Theoretical studies of the effect of deformation on WF suggest that when a crystalline sample is structurally altered, the Fermi energy level would vary, thus leading to changes in WF. An electrostatic interaction model to correlate WF with deformation was proposed, which readily explains the effect of deformation on WF [29]. In the electrostatic interaction model, WF is defined as the depth of the potential well, a one-dimensional lattice is considered. WF can be expressed as:

$$\phi = \sum_{-n}^{n} \frac{ze^2}{4\pi\varepsilon_0 |x_i - x_{ei}|} \tag{19}$$

Where z is the charge number of a nucleus, $\varepsilon_0$is the permittivity constant. x_i and x_{ei} represent the equilibrium position of the nucleus and the position of the electron between x_i and x_{i-1} in the shallowest electron potential well, respectively.

In the elastic deformation region, if a lattice is in tension, the spacing between nuclei as well as that between nuclei and electrons is increased. As a result, WF will decrease according to *Eq. (19).* The result is reversed if the lattice is in compression. If the material suffers from plastic deformation and dislocations are generated, it can be proved that WF decreases based on relevant analysis of *Eq. (19)* and dislocation models.

It is known that dislocation density directly depends on strain [8], so any increase in strain or strain rate can lead to an increase in dislocation density. The WF of various metals and alloys under tensile deformation conditions was measured to study its relations in [37]. With a particular interest in the response of the WF to the deformation type (tension) and the deformation condition (strain rate). According to these experiments [37], the essential effects

of strain and strain rate are to promote the level of dislocation density. Accordingly, an increase in strain or strain rate necessarily decreased the WF, rising the conjecture that dislocations can impact the WF.

1.5.2.1.3 Influences of atomic bond energy in the electron work function

Lennard-Jones(L-J) potential is a mathematically simple model to represent the interaction between a pair of atoms and associated bond energy [38]. Due to its simplicity, the L-J potential has been often used in physical calculation and many material properties can be easily related to the atomic bond energy through the L-J potential [31]. A common expression of Lennard-Jones potential is:

$$V(r) = \varepsilon_b \left[\left(\frac{r_e}{r}\right)^{12} - 2\left(\frac{r_e}{r}\right)^{6} \right] \tag{20}$$

Where ε_b is the depth of the potential well (the bond energy), and r_e is the equilibrium distance between a pair of adjacent atoms. If it is considered that two adjacent atoms are connected by a spring with a spring constant of k, in the vicinity of r_e Taylor expression of the L-J potential is [31]:

$$\begin{aligned} V(r) &= V(r_e) + \frac{V'(r_e)}{1!}(r - r_e) + \frac{V''(r_e)}{2!}(r - r_e)^2 + \cdots \\ &\approx V(r_e) + \frac{1}{2}V''(r_e)(r - r_e)^2 \end{aligned} \tag{21}$$

$$k = \left.\frac{d^2V}{dr^2}\right|_{r-r_e} = \frac{72\varepsilon_b}{r_e^2} \tag{22}$$

Therefore, the spring force (F) and Young's modulus (E) can be calculated as:

$$\mathrm{F} = k\Delta\mathrm{r} = k(\mathrm{r} - r_e) \tag{23}$$

$$\mathrm{E} = \frac{\sigma}{\varepsilon} \tag{24}$$

Where $\sigma$and ε are stress and strain. If it is considered that each atom occupies an area of r_e^2, thus as described in [31]:

$$\sigma = \frac{F}{r_e^2} = \frac{k\Delta\mathrm{r}}{r_e^2} = E \cdot \varepsilon = E\left(\frac{\Delta\mathrm{r}}{r_e}\right) \tag{25}$$

$$\Delta E = \frac{k}{r_e} = \frac{72\varepsilon_b}{r_e^3} \propto \frac{\varepsilon_b}{r_e^3} \tag{26}$$

Since the L-J potential is an inter-atomic pair potential, influences of crystallographic orientations and planes on properties of a solid can be analyzed using the L-J approach as long as (ε_b , r_e) are determined based on the structure and properties of the solid. However, if there is a structural change, corresponding to changes in the electron density and thus WF, these

parameters would be influenced. Thus, (ε_b , r_e) need to be re-determined or re-calculated based on some measured properties of the new structure.

If a material has a higher WF, greater energy is required to change its electron state. For instance, metals having a higher WF possess stronger atomic bonds, corresponding to higher Young's modulus and, stronger bonds also make dislocation activation harder, leading to increased hardness. Moreover, a higher WF corresponds to higher surface energy. Therefore, WF reflects the stability of the electron state or the difficulty to break an atomic bond.

1.5.3 Work function in semiconductors

In semiconductors valence band and conduction band are separated by the bandgap (E_{gap}). In a semiconductor, the FL is located within the bandgap. This means the work function is now different from the ionization energy (energy difference between valence bands maximum and vacuum level). In a semiconductor, the FL becomes a somewhat theoretical construct since there are no allowed electronic states within the bandgap.

Therefore, another concept needs to be defined: electron affinity. In the field of solid-state physics, for a semiconductor-vacuum interface (that is, the surface of a semiconductor), the electron affinity χ is defined as the energy obtained by moving an electron from the vacuum (E_{vac}) just outside the semiconductor to the bottom of the conduction band just inside the semiconductor (E_C) [39]:

$$\chi = E_{vac} - E_C \tag{27}$$

The electron affinity of a surface is closely related to, but distinct from, its work function. Furthermore, while the work function of a semiconductor can be changed by doping, the electron affinity ideally does not change with doping and so it is closer to being a material constant. However, like workfunction, the electron affinity does depend on the surface termination (crystal face, surface chemistry, etc.) and is strictly a surface property [39].

Taking all of this into consideration the work function of semiconductors can be rewritten as:

$$\phi_{theo} = \chi + E_C - E_F \tag{28}$$

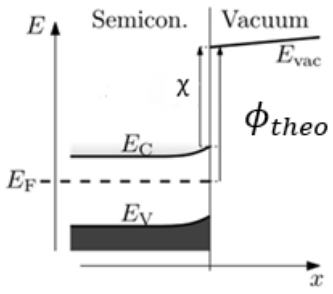

Figure 4: Band diagram of the semiconductor-vacuum interface showing electron affinity χ, defined as the difference between near-surface vacuum energy E_{vac}, and near-surface conduction band edge E_C. Also shown: Fermi level E_F, valence band edge E_V, theoretical work function ϕ_{theo}. Adapted from: [39].

Since the Fermi Level is a theoretical magnitude, in this project, the semiconductor's WF will be defined as:

$$\phi = E_{gap} + \chi \tag{29}$$

Where E_{gap} is defined as:

$$E_{gap} = E_C - E_V \tag{30}$$

Therefore, in order to emit an electron, the energy source must supply this energy to the material:

$$\phi = E_{vac} - E_V \tag{31}$$

Where ϕ is the WF of the semiconductor, the energy difference between Valence energy (E_V) and vacuum level energy (E_{vac}).

1.5.3.1 Influences of temperature, pressure, and strain in semiconductors' electron work function

In the case of dielectrics (insulators) and semiconductors, the bandgap energy is understood to be the width of the energy gap between conduction and valence band. This presence of a bandgap influences the electrical and optical properties. Therefore, the emission properties of these materials are affected. The bandgap in dielectrics is above 4 eV and in semiconductors, it has a smaller width, of only a few electron volts or even less than 1 eV.

The bandgap energy of a semiconductor determines its physicochemical properties, and because of this, a great deal of interest has been devoted to bandgap engineering as a powerful technique for developing new semiconductor materials. Bandgap engineering refers to a process of controlling E_{gap} of a semiconductor, usually adjusted by its chemical composition. Also, the band-gap energy of semiconductors tends to decrease with increasing temperature [40]. When temperature increases, the amplitude of atomic vibrations increases, leading to larger interatomic spacing. This dependence will no longer be treated in this thesis.

However, recent strain-induced bandgap engineering of semiconducting materials has attracted much attention. Although possible strain effects in semiconductors have been investigated for over a half-century, a profound understanding of their influence on energy bands, especially for large elastic strain remains unclear [41].

Like electrons in a semiconductor experience, the periodic potential of the crystal lattice, intrinsic to this structure are several symmetry properties that are influenced by the application of stress [42]. It is known that pressure changes the lattice parameters and therefore average distance between electrons and ions [43] [44]. This results in a change in the magnitude of the electron potential. This modifies the bandwidth, and consequently the bandgap. This effect was studied by A.L. Polyakova [45] with these results:

Table 1: Deformation potential constants

Semiconductor	E_{gap} **[eV]**	$\gamma = \frac{\Delta E_{gap}}{\Delta P_x} x10^{11} [eV/Pa]$
Si	1.21	-1.5
Ge	0.66	5
GaAs	1.43	12
GaSb	0.67	16

Therefore, as in the past decades, there has been much interest in the pressure dependence of the band gaps of semiconductors since the knowledge of this and its behavior under pressure and temperature would enable the prediction of the overall properties of semiconductors [44] [46].

According to [41] it was noted that, for a semiconductor, the strain can change the band structures, carrier concentrations, and motilities, which may significantly affect the transport properties. These calculations indicated that the electron mobility increases with increasing tensile strain and decreases with increasing compressive strain, however, the electron concentration varied slightly with both tensile and compressive strains. This indicates that the change of resistivity mainly results from the variation of electron mobility not to electron concentration.

1.5.4 Influences of crystal defects in the electron work function

In the first half of the last century, it became clear that both plastic and fracture properties of crystals are facilitated by imperfections in the crystal. Similarly, theoretical estimates showed that the fracture of a crystal, which ultimately depends on rupturing interatomic bonds, is a nearly impossible process without the existing imperfections in the crystal. The type of defects for plastic deformation and fracture of a crystal are different; at moderate temperatures yielding is primarily carried forward by linear defects, i.e., dislocations, while the fracture is facilitated by the existence of microscopic bulk defects, e.g., voids or microcracks [47].

Semiconductors are a class of materials that are primarily covalent although the compound semiconductors have a component of ionic bonding that can be quite large. In a covalent crystal, the motion of dislocations involves breaking and re-forming interatomic bonds. Thus, because of their strong covalent/ionic bonds, semiconductors have exceptionally large lattice resistance that makes dislocation motion in them intrinsically difficult. In the fracture of a material, the relevant defects are micro cracks where their role is to concentrate and magnify the applied stress at the crack front to values exceeding the ideal strength of the crystal, i.e. to values required to rupture the interatomic bonds.

2. METHODOLOGY

This thesis aims to perform a computer simulation of the electron emission process while the materials undergo tensile stress using Matlab software. Therefore, a model will be developed using all the information described in the literature review chapter. This model will enable us to study this phenomenon and describe the different parameters involved.

In this model, the excitation of the material will be done by stress simulating that the material is under the tensile test, also the simulation will include that the specimen is under photostimulation. Tensile testing is a commonly used test in materials science and engineering. The test procedure is standardized: it requires a sample that is subjected to a controlled tension until failure. In this test, the elongation and the applied force can be directly obtained from the experimental instrumentation. Moreover, some properties can be directly measured via a tensile test such as ultimate tensile strength, breaking strength, maximum elongation, and reduction in area. Also, from these measurements, more properties can be determined: Young's modulus, Poisson's ratio, and yield strength [43].

In this thesis, only uniaxial tensile testing will be studied since it is the most used for obtaining the mechanical characteristics. Furthermore, it simplifies the calculations and the study of the relations between the parameters involved in electron emission.

The photostimulation will be characterized by the photon's energy which will be a variable in the simulation.

During the tensile test, the elongation of the specimen section is recorded against the applied force. The elongation measurement is used to calculate the engineering strain, ε, using the following equation:

$$\varepsilon = \frac{\Delta L}{L_0} = \frac{L - L_0}{L_0} \tag{32}$$

Where ΔL is the change in specimen length, L_0 is the initial specimen length and L is the final length. As it is considered a bar of the original cross-sectional area A_0 under tension. The material is experiencing stress defined to be the ratio of the force to the cross-sectional area of the bar, as well as axial elongation. The force measurement is used to calculate the engineering stress, σ, using the following equation:

$$\sigma = \frac{F}{A_0} \tag{33}$$

Where F is the tensile force, A_0 is the initial nominal cross-section of the specimen and σ is the engineering stress.

It is necessary to identify the connection between the emission current of the materials and the behavior during the test, considering two types of materials: metals and semiconductors. Therefore, two models will be presented and discussed in the next sections.

2.1 Metallic material model

As it has been presented in section *1.5.2.1 Influences in the electron work function of metals*, its WF is affected by material deformation as the free electron density varies with deformation. This is because during deformation, the lattice is in tension and the spacing between nuclei as well as that between nuclei and electrons is increased, therefore the lattice parameter is changed. Since this parameter is changed, the electron density is also affected. Knowing that:

$$\phi = \frac{e^3 m^{1/2} n^{1/6}}{16\sqrt[3]{3}\pi^{5/3} h \varepsilon_0^{3/2}} \tag{15}$$

Where e is the elementary charge, n is the free electron density, m is the electron mass, ε_0 is the vacuum permittivity and h is Planck's constant. As e, m, h and ε_0 are constants, it can be established that to analytically describe the trend of WF in a tensile test they can be reduced to a constant β, following the equation:

$$\phi = \beta \cdot n^{1/6} = 5.36 \cdot 10^{-5} \cdot \ n^{1/6} \tag{34}$$

As discussed, in [35] the expression of the free electron density n in terms of the Fermi energy E_F can be stablished as

$$n = \frac{8\sqrt{2}\pi m_{rel} c^{3/2}}{hc^3}\left(\frac{2}{3}E_F^{3/2}\right) \tag{35}$$

Where m_{rel} is the rest mass of each fermion, h is Planck constant, and c is the speed of light in the medium. In *Table 2* numerical data is presented: Fermi Energy values extracted from [48], free electron density calculated using *Eq. (35)*, WF values extracted from [49], WF calculated with *Eq.(34)*, and the relative error between them.

Table 2: Fermi Energies [48], calculated Free Electron Densities, Work function [49], and calculated Work Function of different metals. Numerical data extracted from [48]and [49].

Element	**Fermi Energy (eV)** [48]	**Free Electron Density** $\boldsymbol{x10^{28}}$ $\left(\boldsymbol{electrons}/\boldsymbol{m^3}\right)$	**Work function (eV)** [49]	**Work function** ϕ_0 **(eV)**	**Relative error (%)**
Li	4.74	4.69	2.90	3.22	11.0
Na	3.24	2.65	2.75	2.93	6.54
Mg	7.08	8.61	3.66	3.56	2.73
Ca	4.69	4.61	2.87	3.21	11.8
Fe	11.1	17.0	4.50	4.00	11.1
Zn	9.47	13.2	4.33	3.82	11.8
Al	11.7	18.1	4.28	4.03	5.84
In	8.63	11.5	4.12	3.74	9.22
Sn	10.2	14.8	4.42	3.90	11.8
Pb	9.47	13.2	4.25	3.82	10.1

Contemplating a specimen of volume V_0 with an electron density of n_0 the total number of electrons *N* will be:

$$N = n_0 V_0 \tag{36}$$

Considering that the total number of electrons in the specimen is a constant and that the metal is undergoing a tensile test, thus, the length of the specimen is increasing producing a variation in the free electron density:

$$N = \Delta n A_0 \Delta L \tag{37}$$

Where A_0 is the initial nominal cross-section of the specimen, Δn is the variation in the free electron density produced by the variation in the specimen length ΔL. It is going to be established that all the specimens are cylindric with an initial length of 100mm and a diameter of 10mm. Therefore, the relationship between elongation and variation of the work function can be obtained since the variation of the free electron density will be known. In this model crystallographic orientation influences on the WF are not going to be discussed. Therefore, knowing that electrons from the material are emitted when they overcome the WF and taking into consideration that the material is under photo-stimulation, the emission current can be described by *Eq. (7):*

$$I \approx (hv - \phi)^m \tag{7}$$

Where hv is the energy of a photon; this parameter is a test variable, ϕ is the metal's WF and m is the power index. Taking into consideration that the emission current will be affected by the increment in length of the specimen and that in a tensile test the length of the specimen is measured directly, that the photon energy will also be controlled by the test specifications and m will be treated as a test variable. Finally, the algorithm will be:

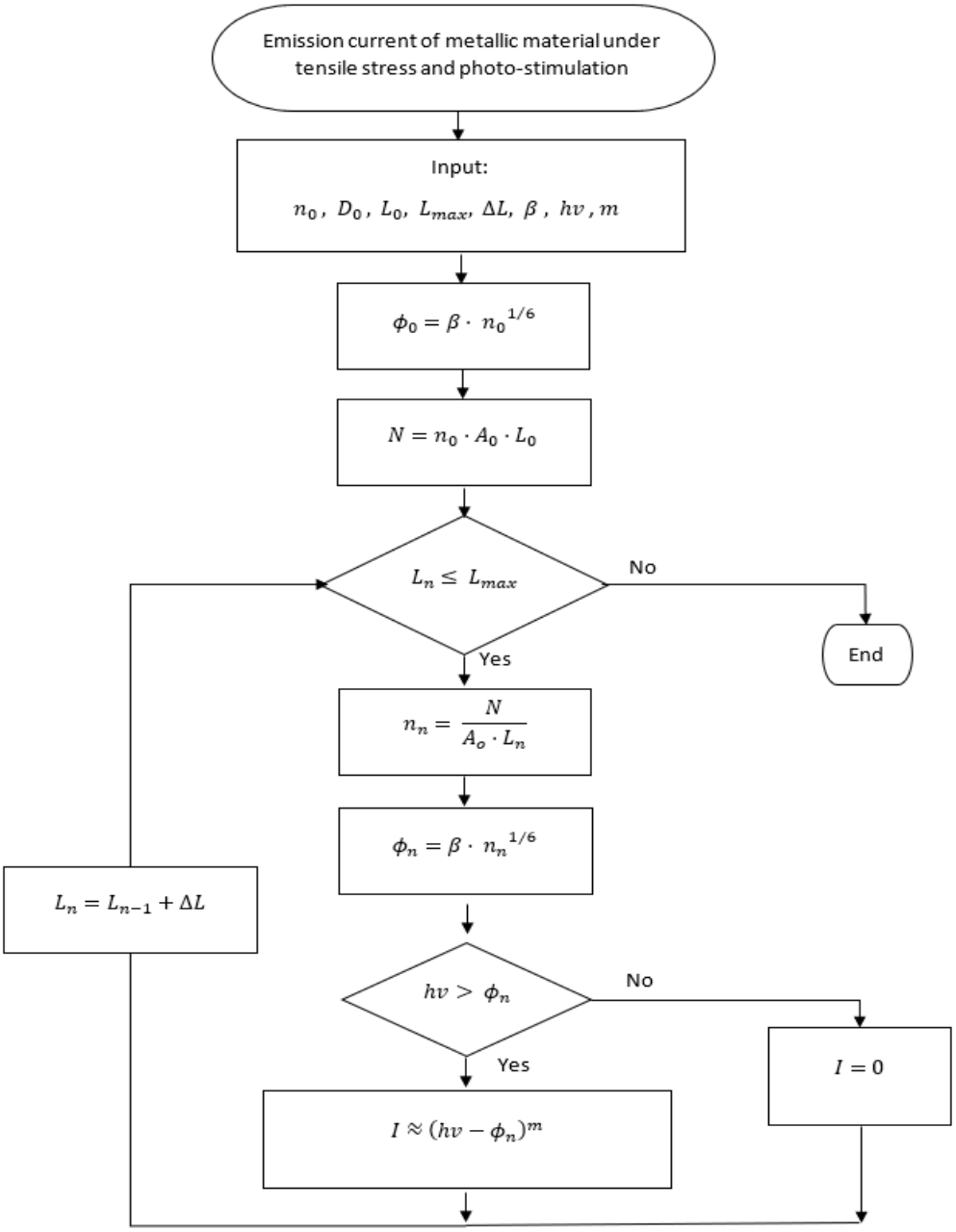

Figure 5: Metallic material algorithm

2.2 Semiconductor material model

Semiconductors have a different electronic structure and thus, a different WF configuration, as it has been presented in *1.5.3 Work function in semiconductors*. Influences in semiconductors' WF that have been studied are focused on temperature variations and pressure variations, some of them produced by strain. Therefore, since the temperature of the test will be established as constant only pressure variations produced by strain will be considered to build the model for this type of materials.

Pressure changes lattice parameters and therefore, the average distance between electrons and ions. Thus, the electronic configuration and the WF are affected by these changes. The

effects of pressure were studied by A.L. Polyakova [45] and the deformation potential constants are presented in *Table 1* with the associated energy gap of the materials, this information has been used to build the model. First, the WF was presented in (29) as:

$$\phi = E_{gap} + \chi \tag{29}$$

In this thesis, as χ depends on the molecular configuration of the material it will be treated as a constant in this model, considering that there is no reconfiguration or recombination of the broken bonds produced by dilatation. When tensile stress is applied to the object it reduces the possibility of recombination of broken bonds by pulling the uncoupled atoms apart [3] [50] [51]. Therefore, the WF variation or will be:

$$\phi_f = E_{gap0} + \Delta E_{gap} + \chi \tag{38}$$

Since the ΔE_{gap} is presented in *Table 1* related to the variations of pressure, knowing that in a tensile test the pressure of the specimen can be obtained as it has been presented in *Eq. (33)* the variations can be calculated sweeping the values of pressure resulted from the test. Being $\Delta\sigma$ the variation in engineering stress, it can be determined that:

$$\Delta\sigma \approx \Delta P_x \tag{39}$$

Then, knowing the variation of stress ΔP_x, the variation in the energy gap can be known using *Table 1*. Thus, the variation of the WF can be solved. Proving that pressure changes the WF.

Also, to have the strain results of the tests it will be established that the semiconductors specimens have the same geometry of metals: all the specimens are cylindric with an initial length of 100mm and a diameter of 10mm.

Therefore, using Hooke's law the relationship between elongation, pressure, and variation of the work function can be obtained. Hooke's law describes that if a material is lightly stressed, a temporary deformation may occur. Removal of the stress results in a gradual return of the material to its original shape and dimensions. Thus, imposing that the tests take place only in the elastic range, the strain will be proportional to stress. Hooke's experimental law may be given by:

$$\sigma = E\,\varepsilon \tag{40}$$

In this model crystallographic orientation influences on the WF are not going to be discussed.

Therefore, knowing the final WF, that electrons from the material are emitted when they overcome the WF, and taking into consideration that the material is under photo-stimulation, the emission current can be described by *Eq. (7).*

$$I \approx (hv - \phi)^m \tag{7}$$

Where hv is the energy of a photon; this parameter will be held constant during the test, ϕ is the variable and m is the power index. Taking into consideration *Eq. (38)* the emission

current can be rewritten as a function of the increment in the energy gap of the specimen material:

$$I \approx \left(hv - \left(E_{gap0} + \Delta E_{gap} + \chi\right)\right)^{m} \quad (41)$$

Finally, to obtain the emitted current, since the photon energy will also be controlled by the test specifications, χ, i.e., the electron affinity and Young's modulus (E) of the material needs to be identified from literature or experimental results.

Table 3: values considered during the simulations.

Semiconductor	$\boldsymbol{E_{gap}}$ **(eV)**	$\frac{\Delta E_{gap}}{\Delta P_x} \boldsymbol{x10^{11}} = \boldsymbol{\gamma}$ $(\boldsymbol{eV/Pa})$	$\boldsymbol{\chi}$ **(eV)**	**Young's modulus (GPa)**
Si	1.21	-1.5	4.05 [52]	160 [53]
Ge	0.66	5	4,00 [50]	140 [54]
GaAs	1.43	12	4,07 [53]	85.5 [56]
GaSb	0.67	16	4,06 [54]	76 [58]

Finally, the algorithm for semiconductor material can be defined as:

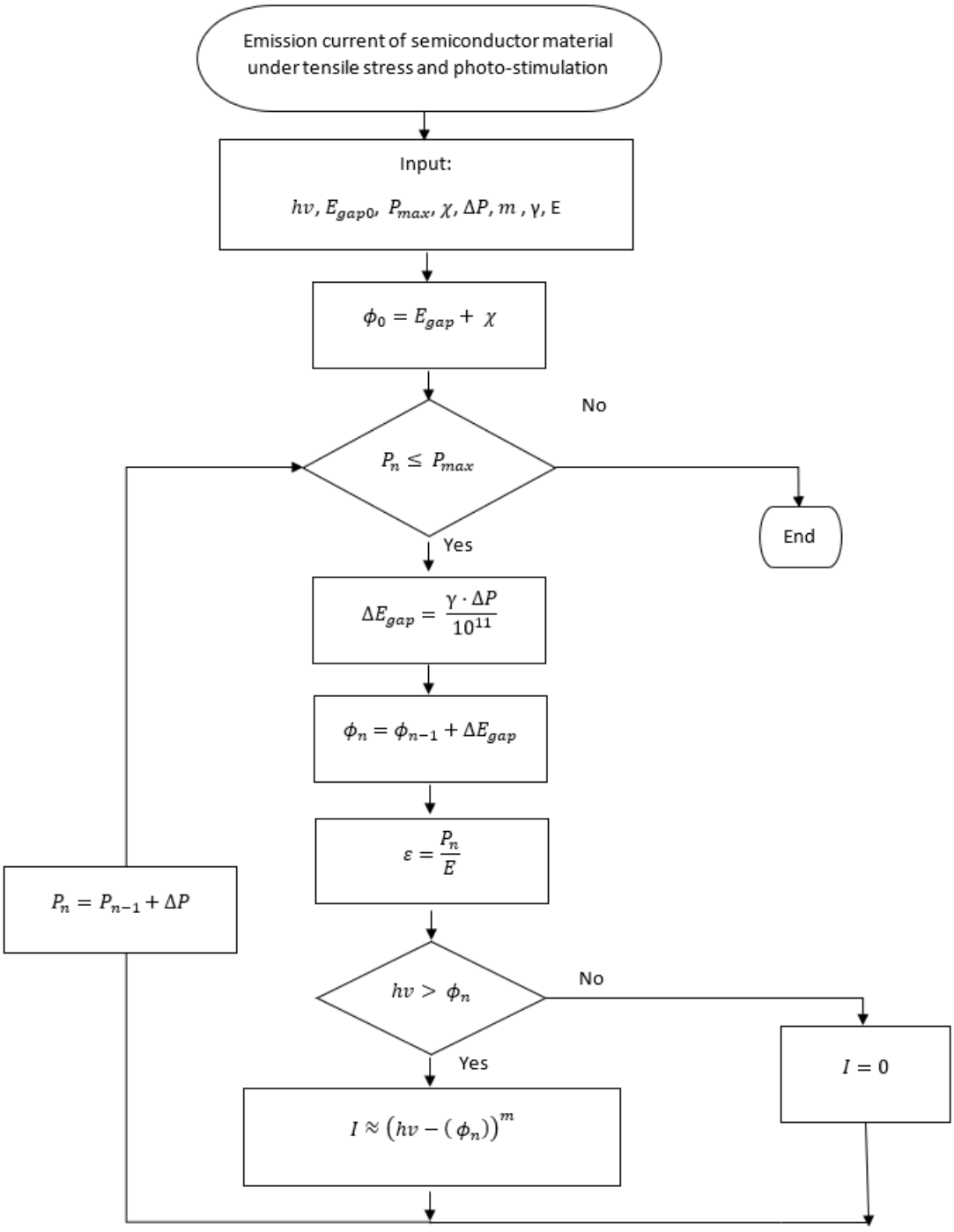

Figure 6: Semiconductor material algorithm

3. RESULTS AND DISCUSSION

3.1 Metals

In this section, metallic material simulation results are presented. There are two different types of results: first, free electron densities and WF variations due to strain. Secondly, the influences of the parameters m and hv are studied, for each metal.

3.1.1 Lithium

According to [55] the failure strain of metallic lithium takes place at 0.35 of strain. Therefore, this was considered as the maximum strain of the specimen and was used to calculate the WF variation of Li with the model presented, obtaining that the WF will decrease 157 meV.

Table 4: Lithium results

	Initial value	Final value	Variation (%)
ϕ (eV)	3.22	3.06	-4.88
n (electrons/m^3)	4.69 x10^{28}	3.47 x10^{28}	-25.9
Length (m)	0.1	0.135	35

As the WF of Lithium is 3.22 eV the photon energy needs to be higher than this value to permit electrons to escape from the surface barrier. Therefore, the analysis has been made with different values of m and hv:

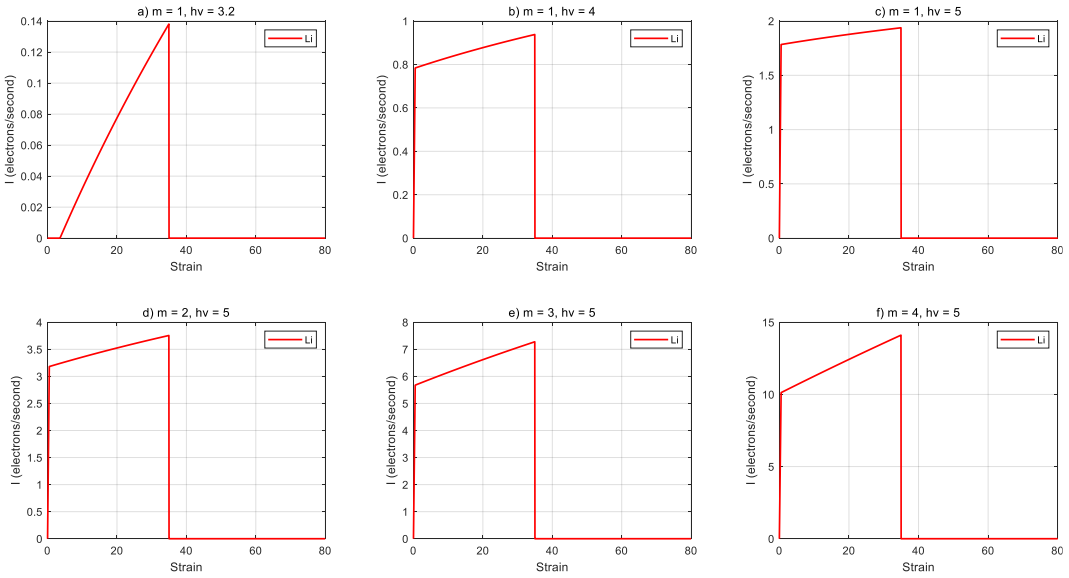

Figure 7: Lithium emission current results a) m=1 and hv=3.2, b) m=1 and hv=4, c) m=1 and hv=5, d) m=2 and hv=5, e) m=3 and hv=5, e) m=3 and hv=5, f) m=4 and hv =5

As it can be observed in *Figure 7 a)* there is no initial emission for $hv = 3.2$ until the WF has decreased enough to allow electrons to escape. In all the other cases as the photon energy is higher than the WF the emission starts immediately. It can also be observed that as bigger as the photon energy is, more electrons are emitted. Also, cases d), e) and f) show the influence of the power index m illustrating that emission grows exponentially as the power index increases, reaching a maximum emission just before the rupture, of 14 electrons/second with $m = 4$ and $hv = 5$. The influences of the parameter m can also be observed in *Figure 8*, where hv is maintained constant. Also, the non-linear tendency of the emission can be observed.

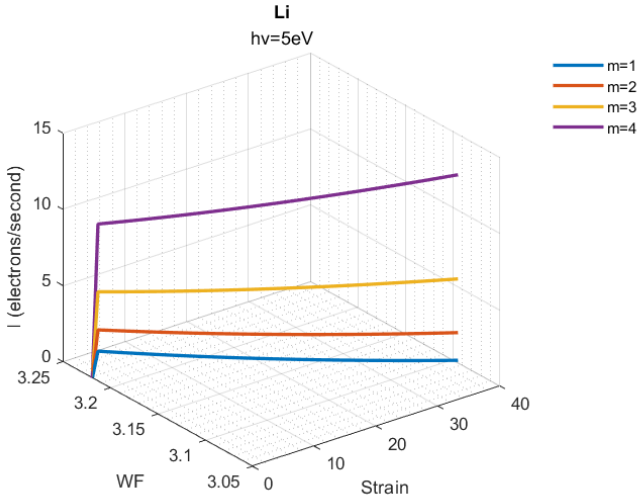

Figure 8:Influence of parameter m in Li

3.1.2 Sodium

As discussed in [56] because of its low melting temperature, the deformation of Na is highly influenced by creep. Under tension, a linear response to loading can be first observed in the low strain region before transitioning to non-linear plastic behavior. In the same study, for comparison with the engineering stress-strain behavior, the true stress-strain curves were calculated. It was found that true stress initially fit well with engineering stress in the low stress-strain region, but it is deviated from the engineering stress after around 3% strain. For the higher strain region in tension, the increase in true stress results from the decreased area under the load caused by necking. Therefore, to study electron emission and taking into account that the model is constructed considering that the area is constant, the maximum strain for the calculations has been established as 3%. Thus, the reduction on the WF has been 14meV.

Table 5: Sodium results

	Initial value	Final value	Variation (%)
ϕ (eV)	2.93	2.91	-0.49
n (electrons/m^3)	2.65 x10^{28}	2.57x10^{28}	-2.91
Length (m)	0.1	0.103	3

The results with different values of m and hv are:

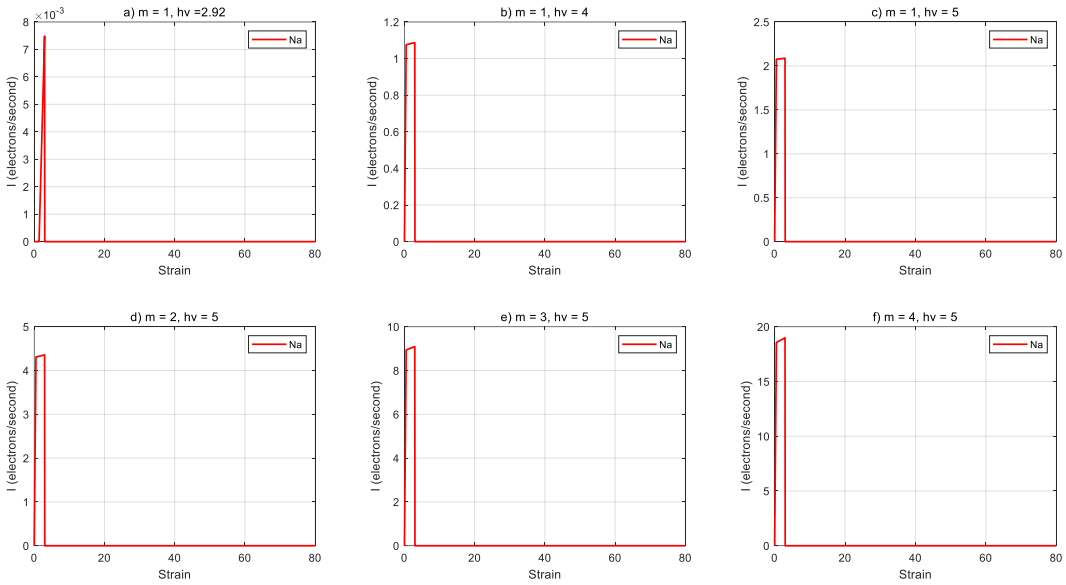

Figure 9: Sodium emission current results a) m=1 and hv=2.92, b) m=1 and hv=4, c) m=1 and hv=5, d) m=2 and hv=5, e) m=3 and hv=5, e) m=3 and hv=5, f) m=4 and hv =5

Figure 9 illustrates the emission process of Sodium. As the maximum strain is only 3% the emission is not maintained for a long period. Despite it is a narrow interval the same tendencies can be observed: there is no initial emission for $hv = 2.92$ until the WF has decreased enough to allow electrons to escape. In all the other cases as the photon energy is higher than the WF the emission starts immediately. Again, as bigger as the photon energy is more electrons are emitted, and as the power index m increases, the emission grows exponentially. In this case, the maximum emission is also just before the rupture, of 19 electrons/second with $m = 4$ and $hv = 5$.

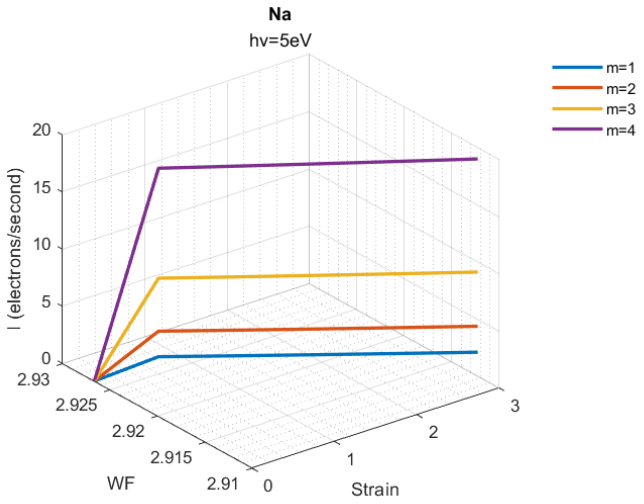

Figure 10: Influence of parameter m in Na

3.1.3 Magnesium

Magnesium materials are supplied in various compositions including commercially pure metal (99.8 % minimum), alloys for casting, and alloys for the manufacture of products. Substantially pure magnesium finds practically no use in engineering design or for stressed applications. The yield strength of the pure metal is about 20 MPa with an elongation of 6 %, and Brinell hardness of 30 [57]. Correspondingly, this elongation was applied to the model, the WF variation was 34 meV.

Table 6: Magnesium results

	Initial value	Final value	Variation (%)
ϕ (eV)	3.56	3.53	-0.97
n (electrons/m^3)	8.61 x10^{28}	8.12x10^{28}	-5.66
Length (m)	0.1	0.106	6

The variation in Magnesium WF is again very narrow. The results with different values of m and hv are:

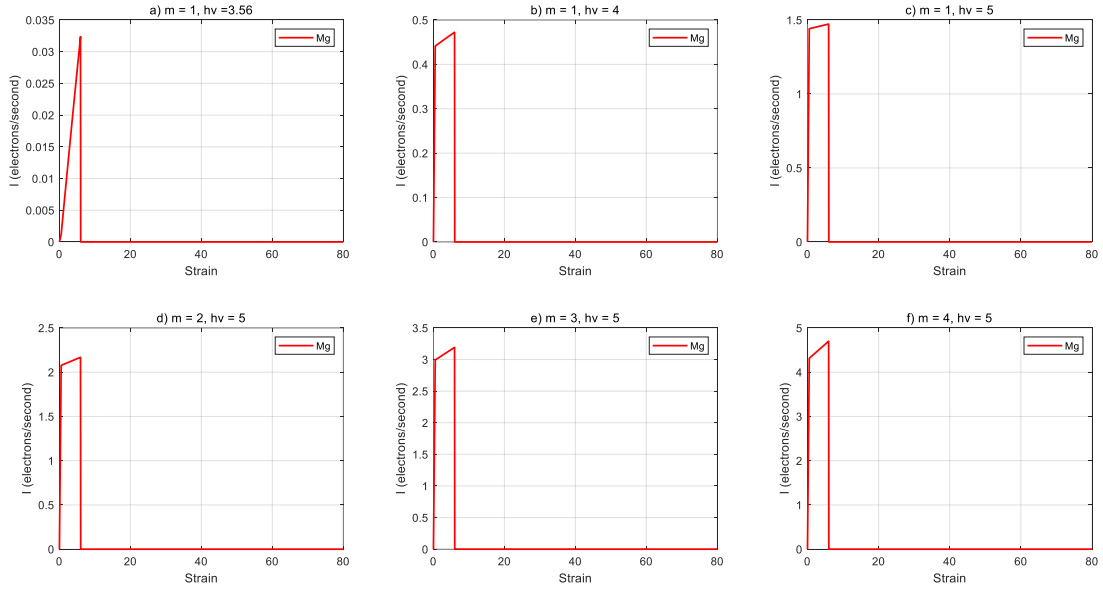

Figure 11: Magnesium emission current results a) m=1 and hv=3.56, b) m=1 and hv=4, c) m=1 and hv=5, d) m=2 and hv=5, e) m=3 and hv=5, e) m=3 and hv=5, f) m=4 and hv =5

Figure 11 illustrates the emission process of Magnesium. As the maximum strain is only 6% the emission is not maintained for a long period. In this case, it can be observed that the emission starts when the photon energy is higher than the WF, and the emission increases with strain. Again, the same tendencies can be observed: as bigger as the photon energy is more electrons are emitted and the power index boosts exponentially the emission as it increases. In this case, the maximum emission is also just before the rupture: of 4.7 electrons/second with $m = 4$ and $hv = 5$. The influences of the parameter m are plotted in *Figure 12* where the strain is not large enough to observe the non-linearity.

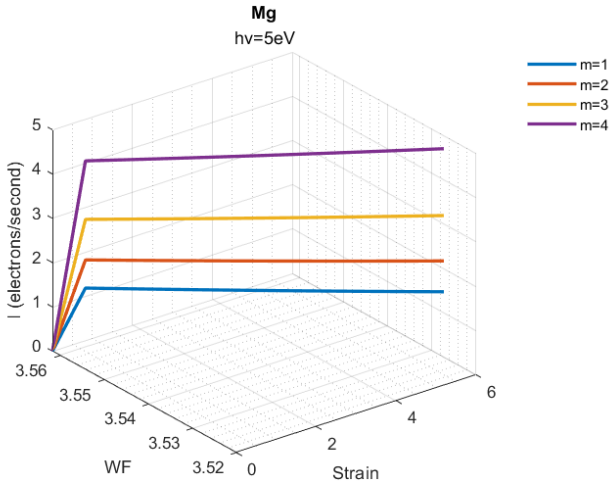

Figure 12:Influence of parameter m in Mg

3.1.4 Calcium

In [58] the tensile properties of swaged and annealed high-purity Ca metal were measured using both constant strain rate tests and strain-rate jump tests. Considering the results of the constant strain rate tests the average elongation of swaged Ca tested at 295 K is 17%. This value has been considered in this study, resulting in a WF variation of 83 meV.

Table 7: Calcium results

	Initial value	Final value	Variation (%)
ϕ (eV)	3.21	3.13	-2.58
n (electrons/m^3)	4.61 x10^{28}	3.94x10^{28}	-14.5
Length (m)	0.1	0.117	17

Calcium WF's initial value is 3.21eV so this will be the first value to study its emission under photostimulation and strain. The results with different values of m and hv are:

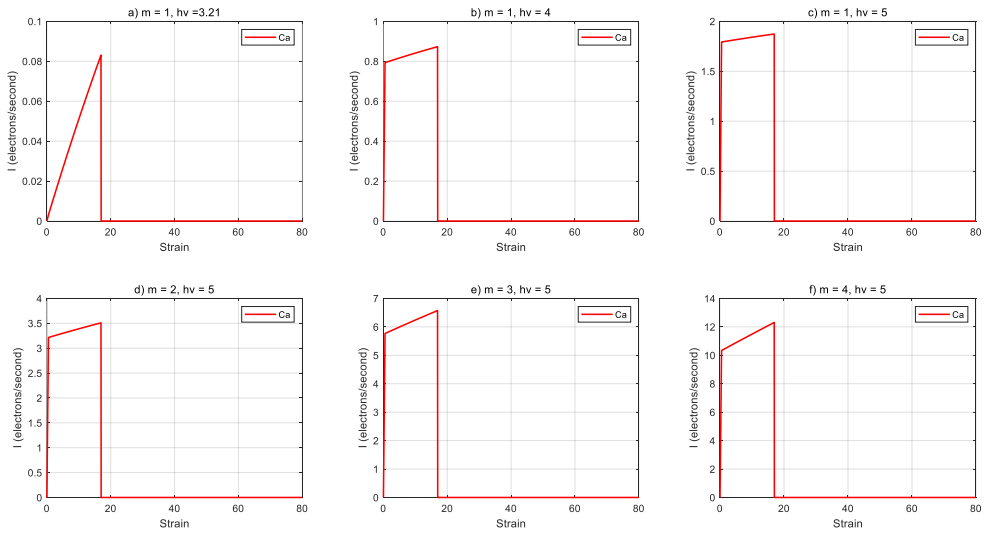

Figure 13: Calcium emission current results a) m=1 and hv=3.21, b) m=1 and hv=4, c) m=1 and hv=5, d) m=2 and hv=5, e) m=3 and hv=5, e) m=3 and hv=5, f) m=4 and hv =5

Figure 13 illustrates the emission process of Calcium. In this case, as the initial photon energy is equal to the WF the emission increases slowly since the first moment, as it can be seen in case a). Again, the emission in all the rest of the cases is instantaneous, and increases with strain, with different initial values accordingly to the different photon's energy. Once again, the same tendencies can be observed: as bigger as the photon energy is more electrons are emitted and the power index boosts exponentially the emission as it increases. In this case, the maximum emission is also just before the rupture, of 12.3 electrons/second with $m = 4$ and $hv = 5$. In *Figure 14* the non-linearity of emission can also be perceived with different values of parameter m.

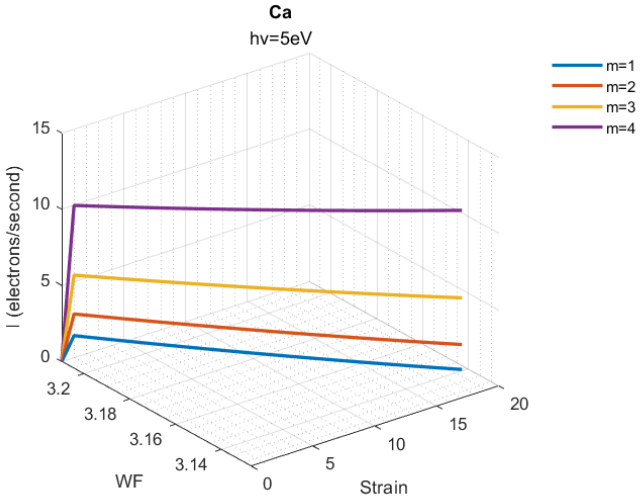

Figure 14: Influence of parameter m in Ca

3.1.5 Iron

In [59] the characterization of room temperature tensile properties of Fe with different degrees of purity, ranging from commercial purity (CP) to ultra-high purity (UHP) are analyzed. Accordingly, the maximum elongation of UHP is an average of 67%. With this strain, the WF variation will be 327 meV.

Table 8: Iron results

	Initial value	Final value	Variation (%)
ϕ (eV)	3.99	3.67	-8.19
n (electrons/m^3)	17.0x10^{28}	10.2x10^{28}	-40.1
Length (m)	0.1	0.167	67

Iron has a huge variation in its WF, its initial value is 3.99eV so the energy of the photon needs to be higher than this value. Results with different values of m and hv are:

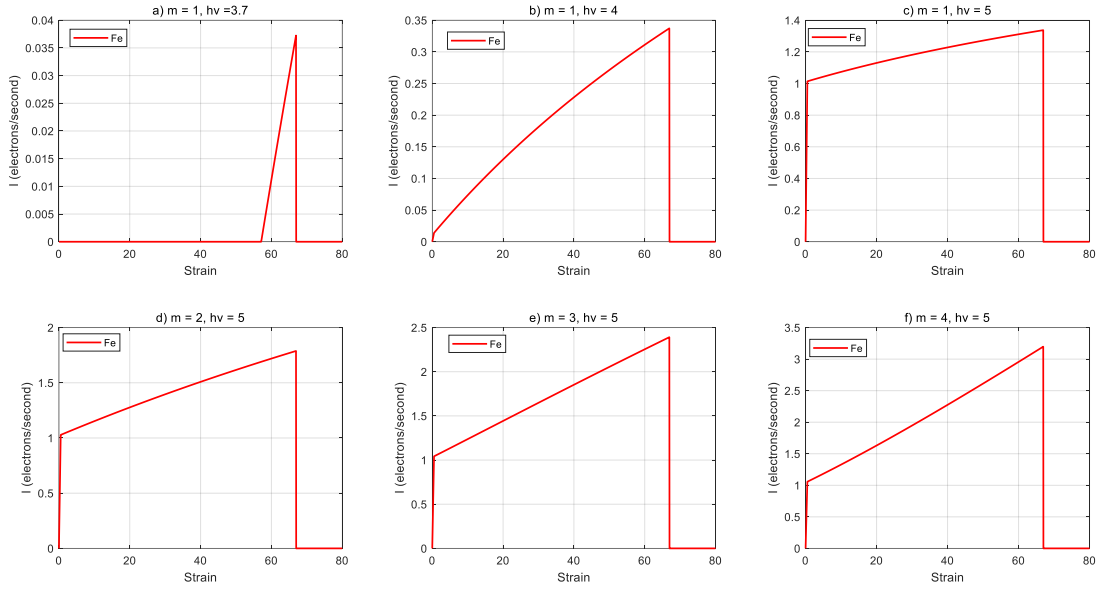

Figure 15: Iron emission current results a) m=1 and hv=3.7, b) m=1 and hv=4, c) m=1 and hv=5, d) m=2 and hv=5, e) m=3 and hv=5, e) m=3 and hv=5, f) m=4 and hv =5

Figure 15 illustrates the emission process of Iron under different cases. As it can be observed in case *a)* the emission only starts when the photon energy is higher than the WF. In the case of b) it can be observed how with $hv = 4$, a value close to the initial WF, the emission current with $m = 1$ shows a non-linear trend. Once again, the same tendencies can be observed: as bigger as the photon energy is more electrons are emitted and the power index boosts exponentially the emission as it increases. In this case, the maximum emission is also just before the rupture, of 3.2 electrons/second with $m = 4$ and $hv = 5$. Moreover, in *Figure 16* the non-linearity can be seen clearly.

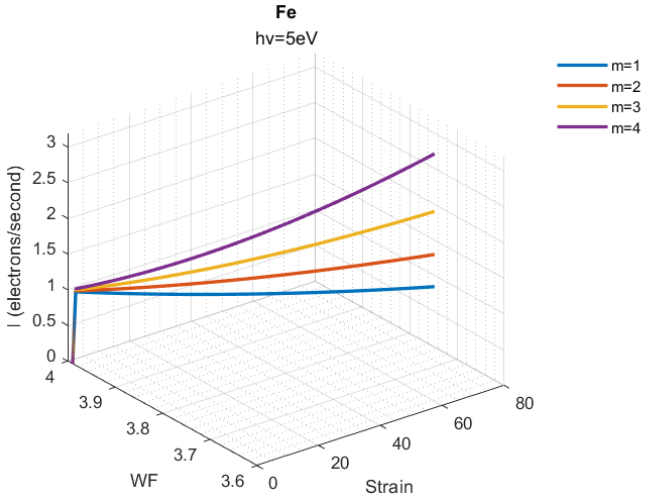

Figure 16: Influence of parameter m in Fe

3.1.6 Zinc

Unfortunately, pure Zn is soft, brittle, and has low mechanical strength in the practice. In [60] the maximum elongation of pure Zn is established to be around 2%. As this material is so brittle the WF is not very affected by deformation. The results are presented in *Table 9:*

Table 9: Zinc results

	Initial value	Final value	Variation (%)
ϕ (eV)	3.82	3.81	-0.33
n (electrons/m^3)	13.2x10^{28}	12.9x10^{28}	-1.96
Length (m)	0.1	0.102	2

The variation of the Zinc Wf is small and also its strain. Nevertheless, to study its emission under photostimulation and strain different values of m and hv are described:

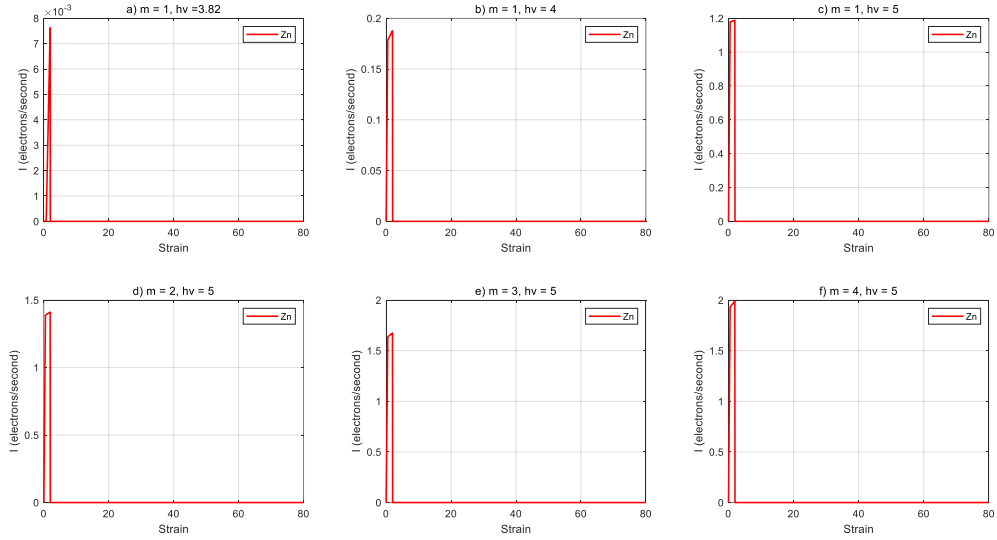

Figure 17: Zinc emission current results a) m=1 and hv=3.82, b) m=1 and hv=4, c) m=1 and hv=5, d) m=2 and hv=5, e) m=3 and hv=5, e) m=3 and hv=5, f) m=4 and hv =5

As it can be observed in *Figure 17* the emission process of Zinc is narrow and the electrons emitted are a minority. Despite this, the same tendencies can be observed. In this material, the maximum emission is just 1.9 electrons/second with $m = 4$ and $hv = 5$. In *Figure 18* for $hv = 5$ and different values of *m*, the same tendencies can be observed.

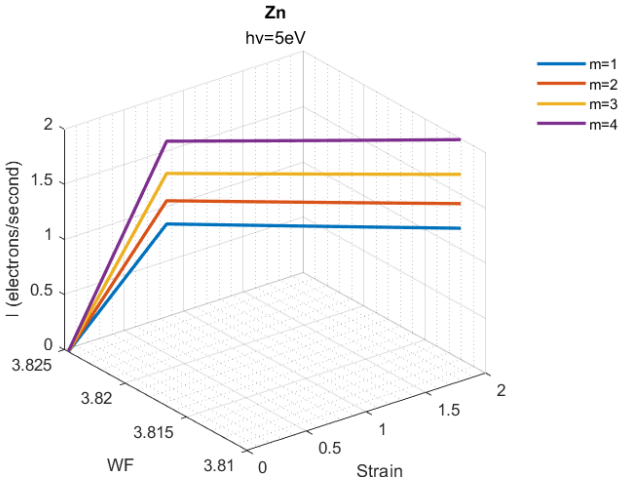

Figure 18: Influence of parameter m in Zn

3.1.7 Aluminum

Pure aluminum is a relatively low strength, extremely flexible metal with virtually no structural applications. In [61] its maximum elongation is established to be 28.8%. Therefore, the results are:

Table 10: Aluminum results

	Initial value	Final value	Variation (%)
ϕ (eV)	4.03	3.87	- 4.13
n (electrons/m^3)	18.1x10^{28}	14.05x10^{28}	- 22.4
Length (m)	0.1	0.129	28.8

Aluminum is a ductile material and the variation of WF is more than 4%. Its emission under photostimulation and strain for different values of m and hv is:

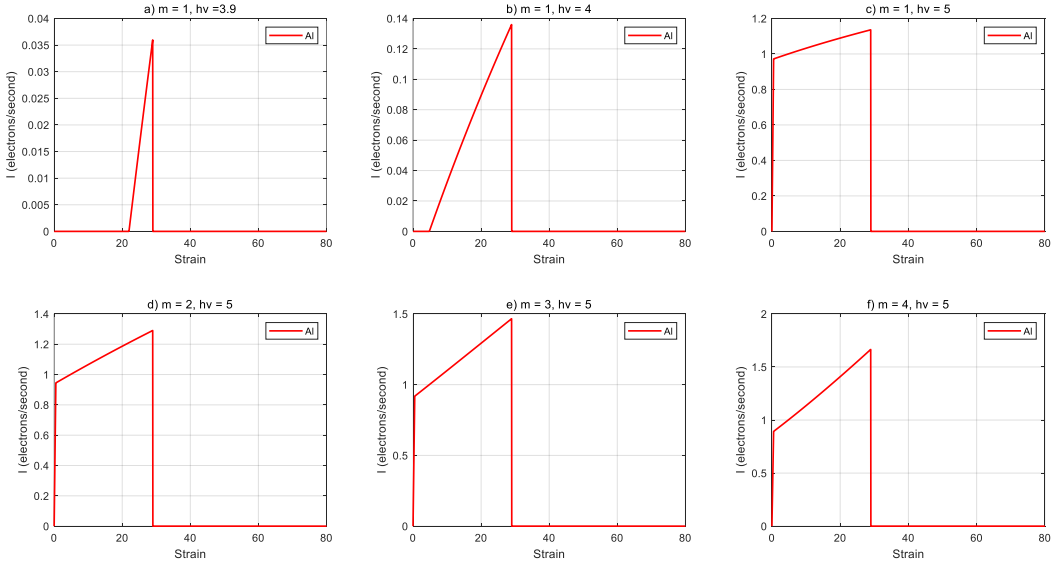

Figure 19: Aluminum emission current results a) m=1 and hv=3.9, b) m=1 and hv=4, c) m=1 and hv=5, d) m=2 and hv=5, e) m=3 and hv=5, e) m=3 and hv=5, f) m=4 and hv =5

Figure 19 illustrates the emission process of Aluminum under different cases, this is remarkably similar to Iron emission despite the Aluminum emission is lower. As it can be observed in cases *a)* and *b)* the emission only starts when the photon energy is higher than the WF. Once again, the same tendencies can be observed. In this case, the maximum emission is also just before the rupture, of 1.7 electrons/second with $m = 4$ and $hv = 5$. In Figure 20 it can be observed how the emission has a non-linear tendency and the variations in the WF are remarkably close at the beginning.

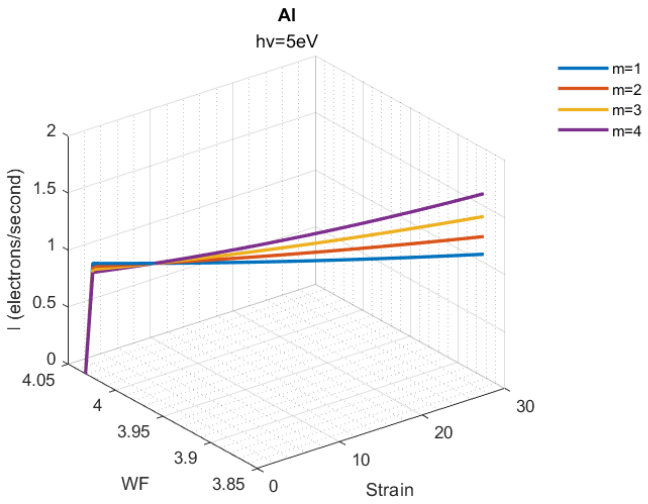

Figure 20: Influence of parameter m in Al

3.1.8 Indium

Indium is a tetragonal, soft, malleable post-transition metal with a melting temperature of only 429 K. If 99.99% pure Indium tested in tensile stress at ambient temperature it is capable of huge elongations (50–70%) that reduce only slightly to around 40–50% at temperatures as low as 4 K. Thus, this metal has huge plasticity [62] Since the reduction in area is not considered in this study the maximum elongation considered will be 20%.

Table 11: Indium results

	Initial value	Final value	Variation (%)
ϕ (eV)	3.74	3.63	-2.99
n (electrons/m^3)	11.5x10^{28}	9.58x10^{28}	-16.7
Length (m)	0.1	0.120	20

The variation in Indium WF is large, being the initial value 3.74eV the photon energy needs to be higher than this in order to see the emission of electrons. The results with different values of m and hv are:

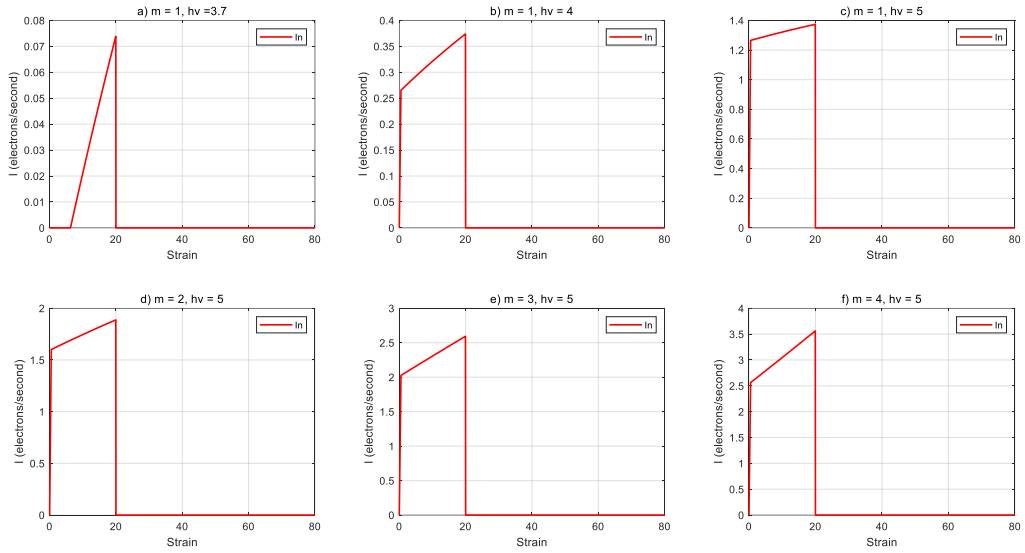

Figure 21: Indium emission current results a) m=1 and hv=3.7, b) m=1 and hv=4, c) m=1 and hv=5, d) m=2 and hv=5, e) m=3 and hv=5, e) m=3 and hv=5, f) m=4 and hv =5

Figure 21 illustrates the emission process of Indium under different cases. Once again, the same tendencies can be observed. In this case, the maximum emission is also just before the rupture, of 3.6 electrons/second with $m = 4$ and $hv = 5$.

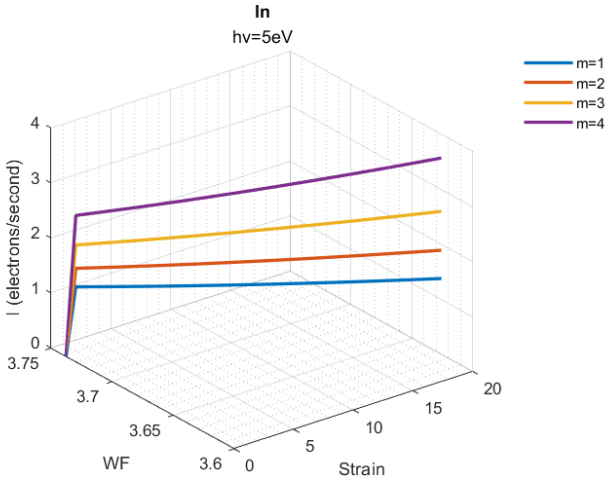

Figure 22: Influence of parameter m in In

3.1.9 Tin

Tin is a soft, malleable, ductile, and highly crystalline metal. According to [63] at room temperature, the maximum strain is 50% with a reduction in the area of 100%. As the reduction in area is not considered in the model, the maximum strain considered will be 10%.

Table 12: Tin results

	Initial value	Final value	Variation (%)
ϕ (eV)	3.89	3.84	-1.58
n (electrons/m^3)	14.8x10^{28}	13.4x10^{28}	-9.09
Length (m)	0.1	0.110	10

The results with different values of m and hv are:

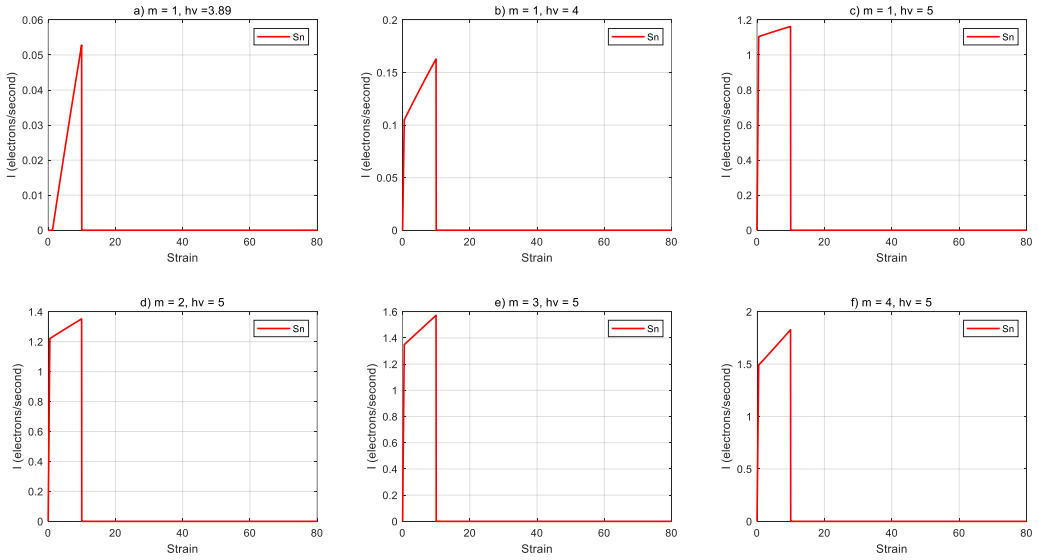

Figure 23: Tin emission current results a) m=1 and hv=3.89, b) m=1 and hv=4, c) m=1 and hv=5, d) m=2 and hv=5, e) m=3 and hv=5, e) m=3 and hv=5, f) m=4 and hv =5

As it can be observed in *Figure 23* and *Figure 24* Tin has the same behavior as other metals studied with a maximum emission current of 1.8 electrons/second with $m = 4$ and $hv = 5$.

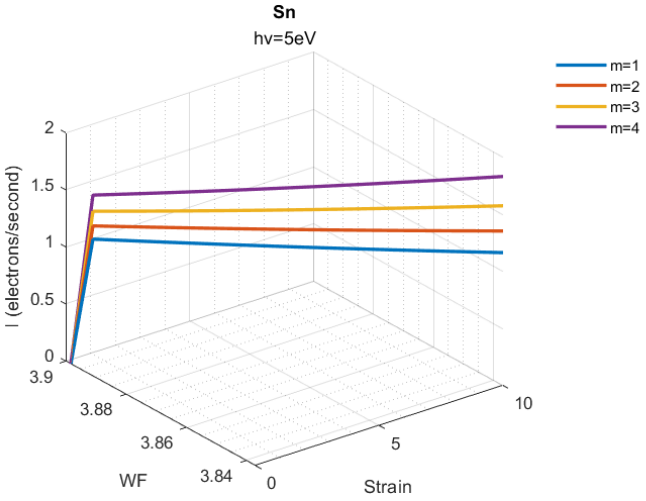

Figure 24: Influence of parameter m in Sn

3.1.10 Lead

Lead is soft and malleable and has a relatively low melting point. According to [64] its maximum strain is 41% on average. As the reduction in area is not considered in this study the maximum elongation considered will be 15%. The WF variation is 88meV.

Table 13: Lead results

	Initial value	Final value	Variation (%)
ϕ (eV)	3.83	3.74	-2.3
n (electrons/m^3)	13.2x10^{28}	11.5x10^{28}	-13.1
Length (m)	0.1	0.115	15

Results with different values of m and hv are:

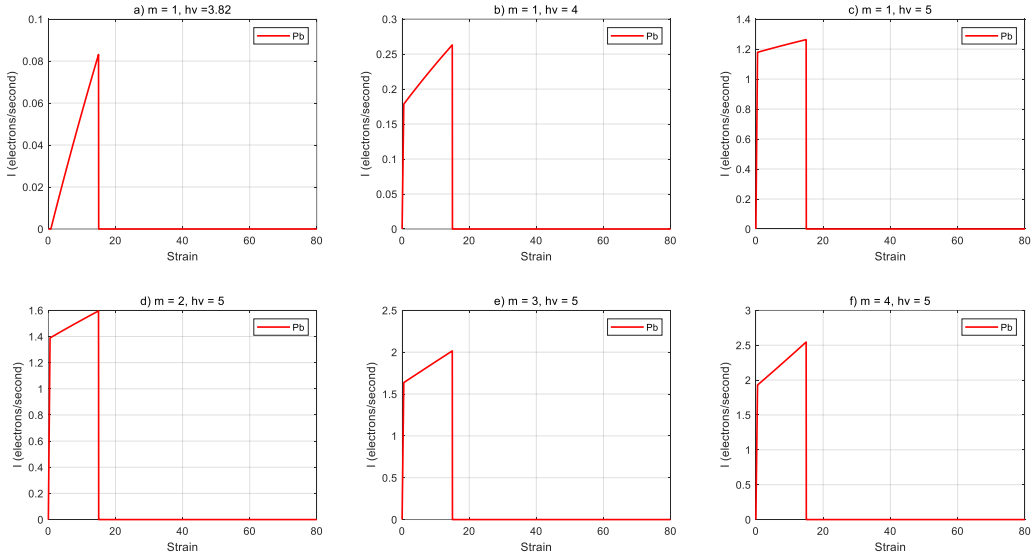

Figure 25: Tin emission current results a) m=1 and hv=3.82, b) m=1 and hv=4, c) m=1 and hv=5, d) m=2 and hv=5, e) m=3 and hv=5, e) m=3 and hv=5, f) m=4 and hv =5

As it can be observed in *Figure 25* Lead has the same behavior as other metals studied with a maximum emission current of 2.5 electrons/second with m=4 and hv=5.

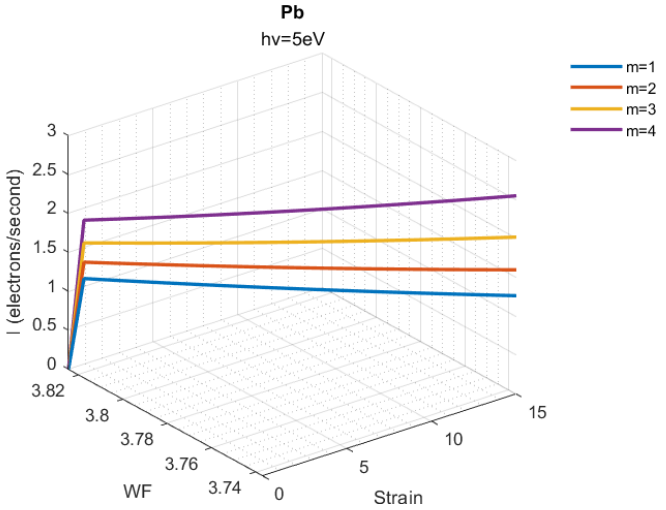

Figure 26: Influence of parameter m in Sn

3.2 Semiconductors

In this section, semiconductor material simulation results are presented. There are two different types of results: first, WF variations due to strain. Secondly, the influences of the parameters m and hv are studied for each semiconductor.

3.2.1 Silicon

The crystal structure of Si belongs to the cubic system of Bravais lattice and consists of two interspersed face-centered cubic lattices. It comprises 8 atoms per unit cell. The basic properties of the crystal structure are reflected in its band structure [42].

The effect of strain on the conductivity of Si was first investigated by Smith [55]. The principal finding of his experimental work was the observation of a change in the Si resistivity on applying uniaxial tensile stress. This change occurs due to a modification of the electronic band structure. Also, [56] discussed how strain changes the lattice, influencing the band structure in two ways: as the volume change it shifts positions of energy bands and the lowering of the crystal-symmetry splits degeneracies in bands. According to results presented in [56], the changes with strain in energy positions of features in the band structure are in the 10–100 meV range.

In [57] a study of strain-induced modulation of the band structure of Si is presented. Since properties of the Si based devices can be modulated by impurities, defects, interfaces, spin, pressure, strain, etc. Concretely, it is said that strain can qualitatively change the photoelectrical and electrophysical properties of Si. Thus, the aim of [57] was to study the electronic structure of Si for different strain values in the range of 0–20 GPa. Thus, it was studied band structure of Si for different values of the lattice parameter, which corresponds to different strain and pressure values. It was found that in the strain range of 0–20 GPa the topmost valence band remains at the point. However, at pressures above 12.5 GPa band structure of Si turns from indirect to direct. Therefore, considering 12.5GPa the maximum pressure the simulation was conducted.

Table 14: Silicon results

	Initial value	Final value	Variation (%)
ϕ (eV)	5.31	5.29	-0.35
E_{gap} (eV)	1.21	1.19	
Length (m)	0.1	0.108	7.8

The results were obtained by sweeping the pressure from 0 to 12.5 GPa. Accordingly, the variation of the WF resulted to be -19 meV, which is in the predicted range of the study [56].

As the WF of Silicon is 5.30 eV the photon energy needs to be higher than this value to permit electrons to escape from the surface barrier. Therefore, the analysis has been made with different values of m and hv:

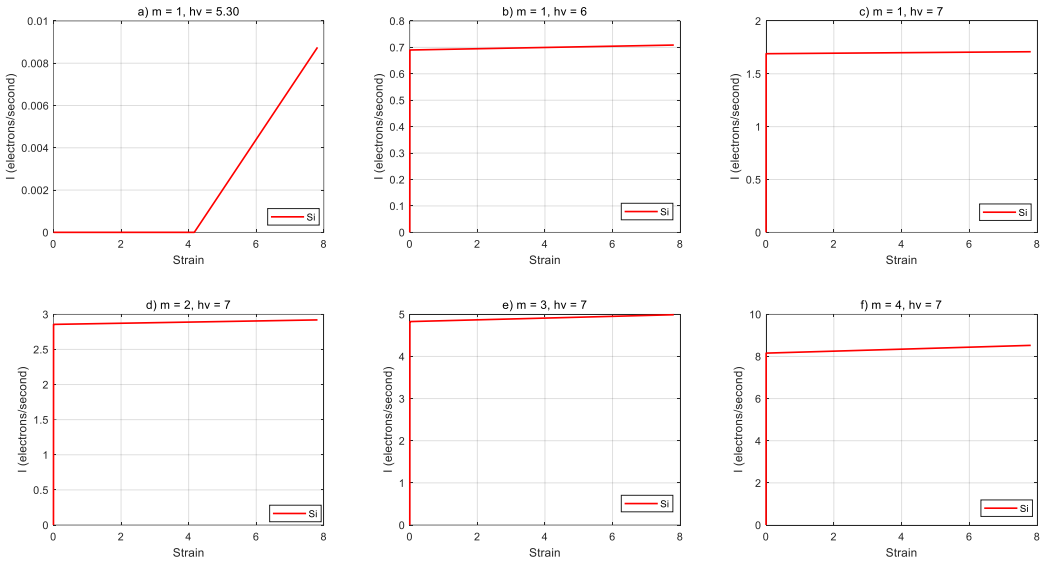

Figure 27: Silicon emission current results a) m=1 and hv=5.30, b) m=1 and hv=6, c) m=1 and hv=7, d) m=2 and hv=7, e) m=3 and hv=7, e) m=3 and hv=7, f) m=4 and hv =7

As it can be observed in *Figure 27* case *a)* there is no initial emission for $hv = 5.30$ until the WF has decreased enough to allow electrons to escape. In all the other cases as the photon energy is higher than the WF the emission starts immediately. It can also be observed that as bigger as the photon energy is more electrons are emitted. Also, cases d), e) and f) show the influence of the power index m illustrating that emission grows exponentially as the power index increases, reaching a maximum emission of 8.52 electrons/second with $m = 4$ and $hv = 7$. In the case of Silicon, the emission tendency is linear as can be observed in *Figure 28*.

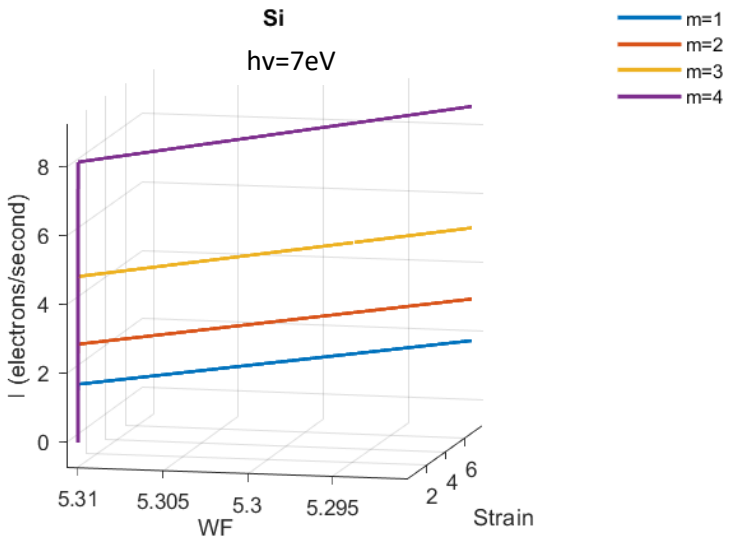

Figure 28: Influence of parameter m in Si

3.2.2 Germanium

Pure Germanium is a hard, lustrous, gray-white metalloid. It has a diamond-like crystalline structure and it is similar in chemical and physical properties to Silicon. Thanks to its electrical properties germanium is used as a semiconductor in transistors and various other

electronic devices. These applications are a function of its band structure which can also be modified. As with Silicon, it is accepted that the band structure of Germanium can be altered by tensile strain. Concretely, in [68] the results of Germanium uniaxially stressed up to 7% longitudinal strain and then performed electro-absorption spectroscopy measurements of energy gap are presented. In this article, it is also described that the bandgap of Germanium suffers an indirect-to-direct bandgap transition at 7%.

In another article [69], the behavior of the bandgap of Germanium is studied until 9 GPa with a variation of approximately 45 meV in the energy gap. Accordingly, our model was applied with a maximum pressure of 9 GPa when the strain has not reached 7%:

Table 15: Germanium results

	Initial value	Final value	Variation (%)
ϕ (eV)	4.66	4.70	0.96
E_{gap} (eV)	0.66	0.70	
Length (m)	0.1	0.106	6.4

The results were obtained by sweeping the pressure from 0 to 9 GPa. Accordingly, the variation of the WF resulted to be 40 meV, which is in the predicted range of the study [69].

As the WF of Germanium is initially 4.66 eV the photon energy needs to be higher than this value to permit electrons to escape from the surface barrier. Therefore, the analysis has been made with different values of m and hv:

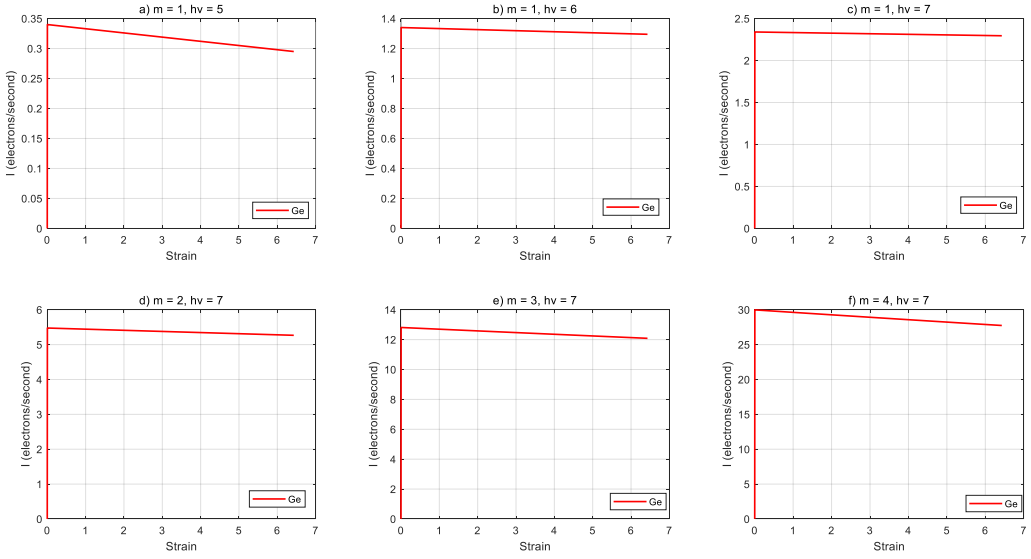

Figure 29: Germanium emission current results a) m=1 and hv=5, b) m=1 and hv=6, c) m=1 and hv=7, d) m=2 and hv=7, e) m=3 and hv=7, e) m=3 and hv=7, f) m=4 and hv =7

As it can be observed in *Figure 29* Germanium has a different behavior because the WF increases with pressure and strain, thus, the emission decreases. In all the cases as the photon energy is higher than the WF the emission starts immediately. It can also be observed that as bigger as the photon energy is more electrons are emitted. Also, cases d), e) and f) show the influence of the power index m illustrating that emission grows exponentially as the power index increases, reaching a maximum emission with lower strains, i.e., at the beginning of the simulation of 30 electrons/second with $m = 4$ and $hv = 7$.

It is seen from *Figure 29* that the WF increases with increasing strain in Ge while decreases with increasing strain in Si (*Figure 27*). In other words, the pressure coefficient (γ) for Si is negative and for Ge is positive. According to [69] the difference in the values of γ depends on the type of transition. The negative value of γ in Si can be explained as the strong influence of the energy levels that lie in energy well above the maxima of the conduction band. These levels repel the conduction band, forcing it downward in energy.

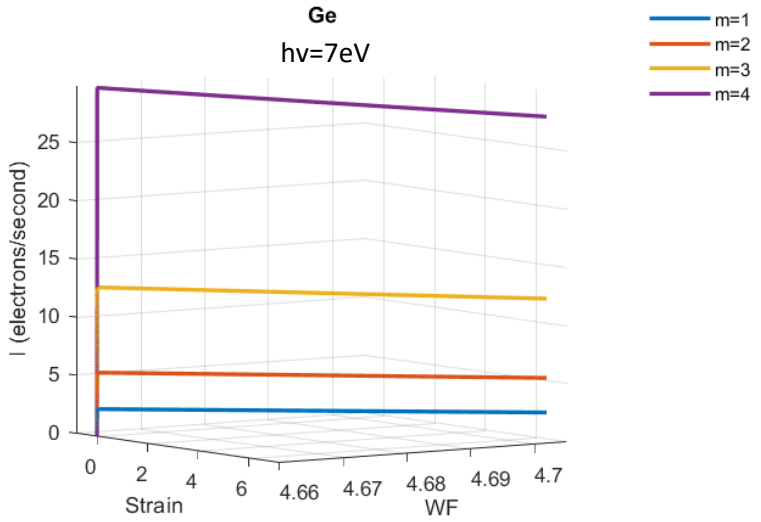

Figure 30: Influence of parameter m in Ge

3.2.3 Gallium arsenide

Gallium arsenide (GaAs) is an III-V direct bandgap semiconductor with a zinc blend crystal structure. Gallium arsenide has high electron mobility therefore, it is used in the manufacture of devices such as infrared light-emitting diodes, laser diodes, solar cells, and optical windows. While it is not truly considered a "wide bandgap" material, GaAs does have a considerably higher bandgap than silicon does. Critically, this makes GaAs highly resistant to radiation and therefore a great choice for defense and aerospace applications. Moreover, GaAs feature a direct bandgap as opposed to silicon's indirect bandgap.

High pressure applied to Gallium Arsenide is a powerful way to induce dramatic electrical conductivity change. Herein, in the study [70] the electrical transport properties of GaAs under high pressure up to 25.0 GPa were analyzed. The experimental results showed that GaAs undergo a semiconductor to metal transition at approximately 12.0 GPa. Accordingly, in [71] the pressure effects on GaAs presented describe that energy gap, valence bandwidth, bulk modulus, and cohesive energy increase with increasing pressure, while the conduction bandwidth decreases. Thus, our model was applied with a maximum pressure of 12 GPa:

Table 16: Gallium arsenide results

	Initial value	Final value	Variation (%)
ϕ (eV)	5.50	5.64	2.62
E_{gap} (eV)	1.43	1.57	
Length (m)	0.1	0.114	14

The results were obtained by sweeping the pressure from 0 to 12 GPa. Accordingly, the variation of the WF resulted to be 144meV, close to the variation found in [72] of 150meV. Therefore, the analysis has been made with different values of m and hv:

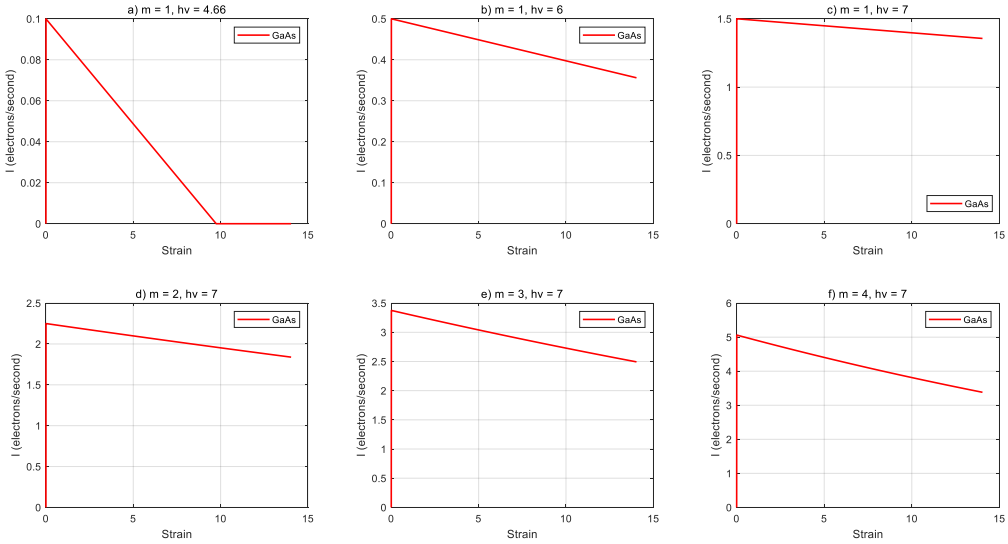

Figure 31: Gallium arsenide emission current results a) m=1 and hv=4.66, b) m=1 and hv=6, c) m=1 and hv=7, d) m=2 and hv=7, e) m=3 and hv=7, e) m=3 and hv=7, f) m=4 and hv =7

As it can be observed in *Figure 31* Gallium arsenide has the same behavior as Germanium, because the WF increases with strain, thus, the emission decreases. It can be observed in case a) where there is electron emission until the WF is higher than 4.66 so at this moment no electrons are emitted from the material. In the rest of the cases as the photon energy is higher than the WF the emission starts immediately. It can also be observed that as bigger as the photon energy is more electrons are emitted. Also, cases d), e) and f) show the influence of the power index m illustrating that emission is boosted as the power index increases, reaching a maximum emission in the first instants of the simulation of case f) of 5 electrons/second with $m = 4$ and $hv = 7$. It can be seen in *Figure 32* that as the parameter *m* increases, the emission current is reduced drastically with strain.

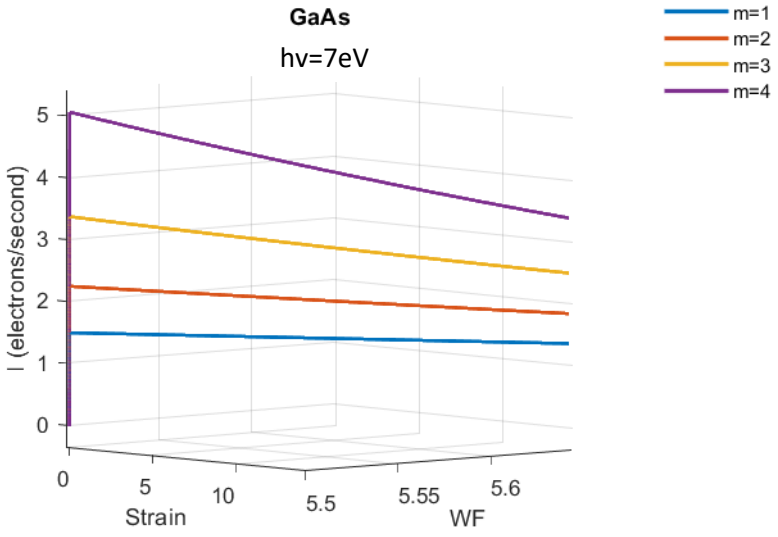

Figure 32: Influence of parameter m in GaAs

3.2.4 Gallium antimonide

Gallium antimonide (GaSb) is a semiconducting compound of gallium and antimony of the III-V family. GaSb can be used for infrared detectors, infrared LEDs and lasers and transistors, and thermophotovoltaic systems.

Research on GaSb under high-pressure presented in [73] explains the behavior of this semiconductor, concretely its metallization. The results provide sufficient evidence for the metallization of the material at 7.0 GPa. As described, at 7.0 GPa, the typical semiconductor behavior of GaSb and accompanying energy barrier disappeared, indicating that GaSB exhibited electronic conductivity, which is characteristic of metal conduction behavior. Moreover, despite no structural transformation was observed before metallization in previous studies; GaSb underwent an electronic structural phase transition from a p-type to an n-type semiconductor at 4.5 GPa. Taking this into consideration the maximum pressure in our simulation will be 4.5 GPa avoiding material transformations.

Table 17: Gallium antimonide results

	Initial value	Final value	Variation (%)
ϕ (eV)	4.73	4.8	1.52
E_{gap} (eV)	0.67	0.74	
Length (m)	0.1	0.106	5.9

The results were obtained by sweeping the pressure from 0 to 4.5 GPa. Accordingly, the variation of the WF resulted to be 144meV, close to the variation found in [72] of 150meV. Therefore, the analysis has been made with different values of m and hv:

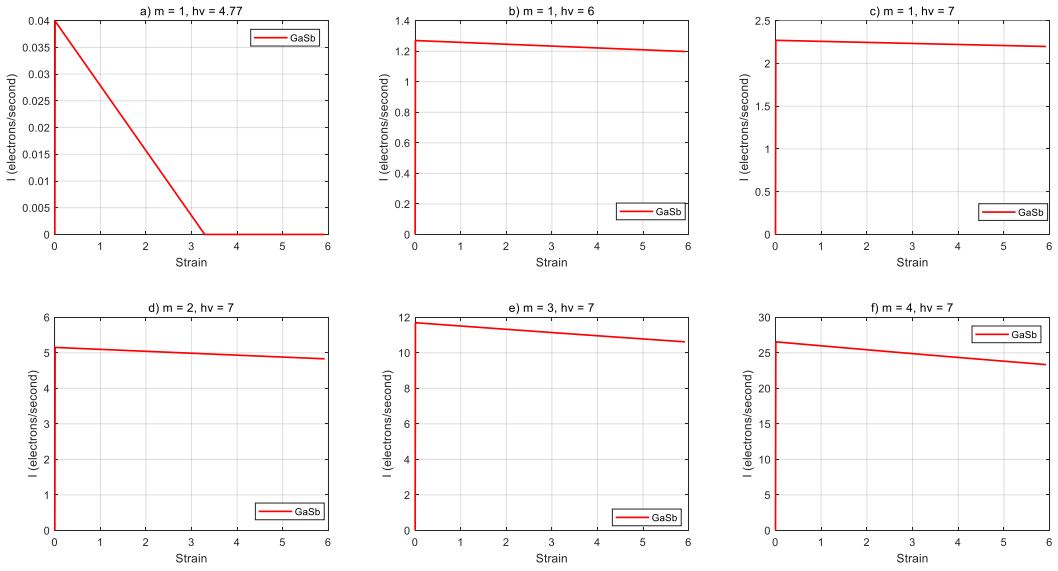

Figure 33: Gallium antimonide emission current results a) m=1 and hv=4.77, b) m=1 and hv=4, c) m=1 and hv=5, d) m=2 and hv=5, e) m=3 and hv=5, e) m=3 and hv=5, f) m=4 and hv =5

As it can be observed in *Figure 33* Gallium antimonide has the same behavior as Germanium and Gallium arsenide, because the WF increases with strain, thus, the emission decreases. It can be observed in case a) where there is electron emission until the WF is higher than 4.77 so at this moment no electrons are emitted from the material. In the rest of the cases as the photon energy is higher than the WF the emission starts immediately. It can also be

observed the same tendency with the photon energy and the power index because if they increase more electrons are emitted at the beginning and it reduces with the increase in m and strain. The maximum emission is reached in the first instants of the simulation of case f) of 26.5 electrons/second with $m = 4$ and $hv = 7$.

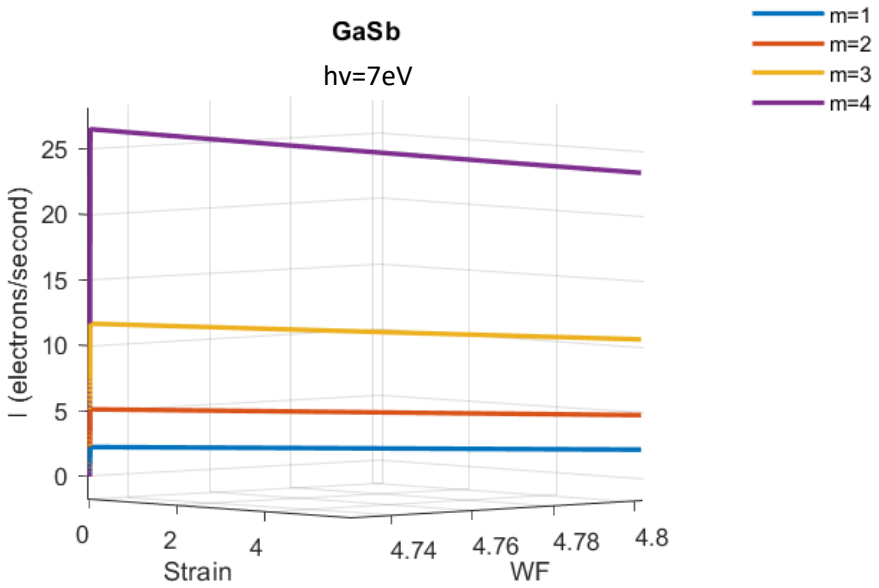

Figure 34: Influence of parameter m in GaSb

Figure 34 shows that the tendency of the emission in the case of semiconductors is linear.

CONCLUSION AND RECOMMENDATIONS

In general terms, in this thesis study, relationships between WF and elongation of atomic bonds have been identified and studied to build simulation models for two types of materials: Metals and Semiconductors. Once the models have been defined, the behavior of this type of materials under strain and photostimulation has been simulated using Matlab. Clear correlations between electron emission and strain have been identified for both types of materials. This demonstrates that WF could be used as a guiding parameter for material characterization and as a predictor of early destruction if more complete models are developed.

Specific conclusions are presented for both types of materials using the simulation results. Concretely, results obtained from the metallic material simulations are resumed in the next table.

Table 18: Metals summary results

Metal	**Initial Work function ϕ_0 (eV)**	**Work function variation (%)**	**Maximum strain (%)**	**Maximum emission current $\left(electrons/_{s}\right)$**
Na	2.93	-0.49	3	19
Ca	3.21	-2.58	17	12.3
Li	3.22	-4.88	35	14
Mg	3.56	-0.97	6	4.7
In	3.74	-2.99	20	3.6
Zn	3.82	-0.33	2	1.9
Pb	3.82	-2.3	15	2.5
Sn	3.90	-1.58	10	1.8
Fe	4.00	-8.19	67	3.2
Al	4.03	-4.13	28.8	1.7

Metallic material results allow us to establish that all the metals present the following characteristics:

- When the photon energy is higher than the WF the emission starts immediately, without strain
- If the photon energy is lower than the WF the emission does not appear
- As bigger as the photon energy is more electrons are emitted
- Power index m boosts emission as it increases with strain, all the metals have their maximum emission just before the rupture. This corresponds with the studied case $m = 4$ and $hv = 5$ for metals
- The maximum emission is reached in Na metal which is the studied material with lower WF despite its elongation is one of the lowest. This corresponds to the validity of the exoemission process where if more energy is given to the electrons, more will be capable to surmount the potential barrier
- The lowest emission is reached in Al, which has the highest WF
- The emission shows a non-linear tendency when strains are considerably large
- The highest reduction of the WF is produced in the case where reached strain is bigger, as WF and strain are inversely proportional due to the electron density
- The photon energy to produce emission in metals has to be in the range of 3-4.5 eV

In total 10 metals have been analyzed, presenting the same tendencies in all of them. Therefore, having reviewed all the literature and after developing the model it can be established that metal's WF is strain-dependent, if a lattice is in tension, the spacing between nuclei as well as that between nuclei and electrons is increased. As a result, WF will decrease according.

Experimental results with this model showed that tensile strain decreased WF. If a material has a higher WF, greater energy is required to change its electron state. For instance, metals having a higher WF possess stronger atomic bonds, corresponding to higher Young's modulus and, stronger bonds also make dislocation activation harder, leading to increased hardness. Moreover, a higher WF corresponds to higher surface energy. Therefore, WF reflects the stability of the electron state or the difficulty to break an atomic bond.

In the case of the semiconductors material model, the results have been:

Table 19: Semiconductors summary results

Semiconductor	**Initial Work function ϕ_0 (eV)**	**Work function variation (%)**	**Maximum strain (%)**	**Maximum emission current $\left(electrons/_{s}\right)$**
Si	5.31	-0.35	7.8	8.5
Ge	4.66	0.96	6.4	30
GaAs	5.50	2.62	14	5
GaSb	4.73	1.52	5.9	26.5

There are two different tendencies observed in the case of semiconductors since Silicon's WF decreases with pressure while all the other semiconductors' WF increases with pressure and strain. Thus, the emission decreases during strain. This is because the pressure coefficient (γ) for Si is negative and for the others is positive because they have different energy transitions. Despite this, the common tendencies are:

- When the photon energy is higher than the WF the emission starts immediately, without strain
- The emission is only possible while the WF is lower than the energy of the photon
- It can also be observed in all the cases that as bigger as the photon energy is more electrons are emitted. This is again in concordance with the principles of the exoemission process
- Also, power index m has the same influence as in metals, boosting the emission as the power index increase. All the semiconductors have their maximum emission in studied case $m = 4$ and $hv = 7$: Silicon at the end of the test and all the others at the beginning, in all the cases where the WF is lower
- The maximum emission is reached in Ge which is the studied material with lower WF
- Contrary, the lowest emission is reached in GaAs, which has the highest WF
- In the case of semiconductors, the emission presents a linear tendency
- Semiconductors need more energy from the photons than metals since the energy supplied to overcome the bandgap has to be higher. The range to generate electron emission should be a minimum of 5.4 eV

In total 4 semiconductors have been analyzed, with two different behaviors according to the sign of the pressure coefficient. Therefore, having reviewed all the literature and after developing the model it can be established that also semiconductor's WF is strain-dependent.

The results obtained, are in particularly good agreement with the existing experimental data, as has been discussed during the thesis. Despite it is recommended to apply it to more tensile-strain experiments in order to clarify the dependencies and establish constant values more accurately. In addition to this, we have found that the parameters involved in the models are physically reasonable. Thus, the results presented are self-consistent and the model can be applied successfully to account for the emission process of different metals and semiconductors. It also could be applied to different materials not studied in this thesis using appropriate parameters.

Finally, this method has shown to give a good description of the emission process under strain and photostimulation of materials and it is expected that this method could give a reliable description for other materials and could be a useful tool to predict materials properties and behaviors.

Further improvements need to be made in the study of the relationship between strain and band structure of materials since our simulation highlight the need for proper experimental verification of the dependence of the band structure on the strain and also, the presence of defects in the materials needs to be assessed.

ACKNOWLEDGMENTS

I would like to thank my supervisors for providing guidance and feedback throughout this project. I am also thankful to the RTU to accepted me as an Erasmus student.

To conclude, I cannot forget to thank my family and friends for all the encouragement and support during all the study years.

REFERENCES

[1] Creative commons wiki, "Material failure theory," January 2020. [Online]. Available: https://en.wikipedia.org/wiki/Material_failure_theory. [Accessed 29 October 2020].

[2] School of Engineering Brown University, "Advanced mechanics of solids," [Online]. Available: https://www.brown.edu/Departments/Engineering/Courses/En1750/Notes/Failure/Failure.htm. [Accessed 29 October 2020].

[3] V. R. Regel, A. I. Slutsker and E. E. Tomashevsk , "The kinetic nature of the strength of solids," *SOVIET PHYSICS USPEKHI*, vol. 15, no. 1, pp. 193-228, 1972.

[4] Editors of Encyclopaedia Britannica, "Crystal defect," October 2006. [Online]. Available: https://www.britannica.com/science/crystal-defect. [Accessed 20 November 2020].

[5] Engineering notes, "4 Main Types of Point Defects in Crystals," [Online]. Available: https://www.engineeringenotes.com/metallurgy/defects-metallurgy/4-main-types-of-point-defects-in-crystals-metallurgy/43090. [Accessed 27 December 2020].

[6] Member of the Collaboration of for NDT Education, "Linear Defects - Dislocations," [Online]. Available: https://www.nde-ed.org/EducationResources/CommunityCollege/Materials/Structure/linear_defects.htm. [Accessed 2 December 2020].

[7] Engineering notes, "Surface Defects in Crystals," [Online]. Available: https://www.engineeringenotes.com/metallurgy/defects-metallurgy/surface-defects-in-crystals-3-types-metallurgy/43279. [Accessed 27 December 2020].

[8] W. D. Callister, Materials Science and Engineering an Introduction, 7 ed., New York City: John Wily and Sons, 2008, p. 905.

[9] E. E. D. &. M. K. P. J. T. Dickinson, "The emission of electrons and positive ions from fracture of materials," *Journal of Materials Science,* no. 16, p. 2897–2908, 1981.

[10] S. Blair, "Band Theory of Metals and Insulators," 11 May 2019. [Online]. Available: https://chem.libretexts.org/Bookshelves/Inorganic_Chemistry/Map%3A_Inorganic_Chemistry_(Housecroft)/06%3A_Structures_and_energetics_of_metallic_and_ionic_solids/6.08%3A_Bonding_in_Metals_and_Semicondoctors/6.8B%3A_Band_Theory_of_Metals_and_Insulators. [Accessed 11 November 2020].

[11] The Editors of Encyclopaedia Britannica, "Band theory," 17 January 2014. [Online]. Available: https://www.britannica.com/science/band-theory. [Accessed 11 November 2020].

[12] Lumen Candela, "Band Theory of Electrical Conductivity," [Online]. Available: https://courses.lumenlearning.com/boundless-chemistry/chapter/band-theory-of-electrical-conductivity/. [Accessed 12 November 2020].

[13] The Editors of Encyclopaedia Britannica, "Metal," 02 June 2020. [Online]. Available: https://www.britannica.com/science/metal-chemistry. [Accessed 27 December 2020].

[14] Creative commons wiki, "Metal," 12 December 2020. [Online]. Available: https://en.wikipedia.org/wiki/Metal#Form_and_structure. [Accessed 14 December 2020].

[15] Vedantu, "Dielectric properties," [Online]. Available: https://www.vedantu.com/physics/dielectric-properties. [Accessed 11 November 2020].

[16] Electrical4U, "Dielectric Materials," 25 October 2020. [Online]. Available: https://www.electrical4u.com/dielectric-materials/. [Accessed 11 November 2020].

[17] S. Holzer, "Dielectrics," 19 11 2007. [Online]. Available: https://www.iue.tuwien.ac.at/phd/holzer/node37.html. [Accessed 11 November 2020].

[18] D. R. Paschotta, "Band Gap," [Online]. Available: https://www.rp-photonics.com/band_gap.html. [Accessed 12 December 2020].

[19] G. Mukhopadhyay, "Effects of mechanical deformation: Exoemission," *Bulletin of Materials Science* , vol. 6, no. 4, pp. 755-772, 1984.

[20] J. E. Davies, "Exoemission for Biomaterials Research," *Japanese Journal of Applied Physics*, vol. 24, no. 43, 1985.

[21] M. C. a. S. C. Langford, "Determination of strain localization in aluminum alloys using laser-induced photoelectron emission," *Journal of Applied Physics* , vol. 96, no. 7189, 2004.

[22] Electrical4U, "Photoelectric Emission," 28 October 2020 . [Online]. Available: https://www.electrical4u.com/photoelectric-emission/. [Accessed 10 November 2020].

[23] Electrical4U, "Work Function: Equation & Relation To Threshold Frequency," 27 July 2020. [Online]. Available: https://www.electrical4u.com/work-function/. [Accessed 17 November 2020].

[24] A. G. a. Y. V. Yu.D. Dekhtyar, "Photo- and exoelectron analysis of the surface," *INT. J. ADHESION AND ADHESIVES*, vol. 14, no. 4, pp. 255-259, 1994.

[25] D. R. Schlaf, "Tutorial on Work Function," [Online]. Available: https://mmrc.caltech.edu/XPS%20Info/TutorialsWorkFunction%20Schlaf.pdf. [Accessed 29 December 2020].

[26] K. Mungole, "What is the work function of a metal and semiconductor?," 2019. [Online]. Available: https://www.quora.com/What-is-the-work-function-of-a-metal-and-semiconductor. [Accessed 13 November 2020].

[27] G. Schirripa Spagnolo, F. Leccese and M. Leccisi, "LED as Transmitter and Receiver of Light: A Simple Tool to Demonstration Photoelectric Effect," 15 October 2019. [Online]. Available: https://www.mdpi.com/2073-4352/9/10/531/htm. [Accessed 13 November 2020].

[28] Y. W. a. D. Y. L. Wen Li, "Response of the electron work function to deformation and yielding behavior of copper under different stress states," *Physica status solidi*, vol. 201, no. 9, pp. 2005-2012, 2004.

[29] W. L. a. D. Y. Li, "Effects of dislocation on electron work function of metal surface," *Materials Science and Technology*, vol. 18, no. 9, pp. 1057-1060, 2002.

[30] G. H. a. D. Li, "The correlation between the electron work function and yield strength of metals," *Applied Physics Letters*, vol. 99, no. 4, 2011.

[31] H. L. a. D. Li, "Correlation between the electron work function of metals and their bulk moduli, thermal expansion and heat capacity via the Lennard–Jones potential," *Physica Status Solidi*, vol. 251, no. 4, p. 815–820, 2014.

[32] X. H. a. D. L. Hao Lu, "Understanding the bond-energy, hardness, and adhesive force from the phase diagram via the electron work function," *Journal of Applied Physics*, no. 173506, p. 116, 2014.

[33] G. H. a. D. L. Hao Lu, "Dependence of the mechanical behavior of alloys on their electron work function—An alternative parameter for materials design," *Applied Physics Letters*, no. 261902, 2013.

[34] Creative commons wiki, "Wigner–Seitz radius," 11 November 2019. [Online]. Available: https://en.wikipedia.org/wiki/Wigner%E2%80%93Seitz_radius. [Accessed 29 December 2020].

[35] R. Nave, "Microscopic View of Ohm's Law," [Online]. Available: http://hydrogen.physik.uni-wuppertal.de/hyperphysics/hyperphysics/hbase/electric/ohmmic.html. [Accessed 30 December 2020].

[36] R. Nave, "Fermi Energies, Fermi Temperatures, and Fermi Velocities," [Online]. Available: http://hyperphysics.phy-astr.gsu.edu/hbase/Tables/fermi.html#c1. [Accessed 30 December 2020].

[37] M. C. Y. W. S. Y. W. Li, "Influences of tensile strain and strain rate on the electron work function of metals and alloys," *Scripta Materialia*, vol. 54, no. 5, pp. 921-924, 2006.

[38] Creative commons wiki, "Lennard-Jones potential," 9 December 2020. [Online]. Available: https://en.wikipedia.org/wiki/Lennard-Jones_potential. [Accessed 10 January 2021].

[39] Wikiwand community, "Electron affinity," [Online]. Available: https://www.wikiwand.com/en/Electron_affinity. [Accessed 10 December 2020].

[40] B. J. V. Zeghbroeck, "2.2.5 Temperature dependence of the energy bandgap," 1997. [Online]. Available: https://ecee.colorado.edu/~bart/book/eband5.htm. [Accessed 10 January 2021].

[41] K. Z. Rui-wen Shao, "Bandgap engineering and manipulating electronic and optical properties of ZnO nanowires by uniaxial strain," *Nanoscale*, vol. 6, no. 4936, 2014.

[42] S. Dhar, "3. Strain Effects on the Electronic Band Structure," [Online]. Available: https://www.iue.tuwien.ac.at/phd/dhar/node16.html. [Accessed 14 January 2021].

[43] Creative commons wiki, "Tensile testing," 26 December 2020. [Online]. Available: https://en.wikipedia.org/wiki/Tensile_testing. [Accessed 30 December 2020].

[44] E. E. A.R. Degheidy, "Effect of pressure and temperature on electronic structure of GaN," Department of Physics, Faculty of Science, Mansoura University, Mansoura, Egypt, 2011.

[45] A. L. Polyakova, Deformation of Semiconductors and Semiconductor Devices, Moscow , 1979, p. 168.

[46] "Pressure dependence of the band gaps of semiconductors," *PHYSICAL REVIEW B*, vol. 40, no. 18, 1989.

[47] P. P. W. Z.-L. Demenet, On the Plasticity and Fracture of Semiconductors, 2004.

[48] N. W. A. a. N. D. Mermin, Solid State Physics, Cornell University, 1976, p. 848.

[49] T. D. Stan Halas, "Work functions of elements expressed in terms of the Fermi energy and the density of free electrons," *Journal of Physics Condensed Matter*, vol. 10, no. 48, 1999.

[50] Creative commons Wiki, "Electron affinity," 22 September 2020. [Online]. Available: https://en.wikipedia.org/wiki/Electron_affinity. [Accessed 11 January 2021].

[51] C. Kittel, Introduction to Solid State Physics, John Wiley & Sons Inc, 2004, p. 704.

[52] openstat, "http://www.ioffe.ru/SVA/NSM/Semicond/Si/basic.html," [Online]. Available: http://www.ioffe.ru/SVA/NSM/Semicond/Si/basic.html. [Accessed 15 January 2021].

[53] MEMS, "Material: Silicon (Si), bulk," [Online]. Available: https://www.memsnet.org/material/siliconsibulk/. [Accessed 11 February 2021].

[54] AZO MATERIALS, "Supplier Data - Germanium (Ge) (Goodfellow)," [Online]. Available: https://www.azom.com/properties.aspx?ArticleID=1837. [Accessed 11 February 2021].

[55] Openstat, "Basic Parameters of Gallium Arsenide," [Online]. Available: http://www.ioffe.ru/SVA/NSM/Semicond/GaAs/basic.html. [Accessed 11 January 2020].

[56] MEMS, "Material: Gallium Arsenide (GaAs), bulk," [Online]. Available: https://www.memsnet.org/material/galliumarsenidegaasbulk/. [Accessed 11 February 2021].

[57] Matprop, "Basic Parameters of Gallium Antimonide (GaSb)," [Online]. Available: http://www.matprop.ru/GaSb_basic. [Accessed 11 January 2021].

[58] R. G. a. F.-X. Coudert, "GaSb (Materials Project id mp-1156)," [Online]. Available: http://progs.coudert.name/elate/mp?query=mp-1156. [Accessed 11 February 2021].

[59] Cole D. Fincher, Daniela Ojeda, Yuwei Zhang, George M. Pharr, Matt Pharr, "Mechanical Properties of Metallic Lithium: from Nano to Bulk Scales," *Acta Materialia*, no. 186, 2019.

[60] J.-Y. C. J. B. W. a. J. S. Michael J. Wang, "Analysis of Elastic, Plastic, and Creep Properties of Sodium Metal and Implications for Solid-State Batteries," *Materialia*, 2020.

[61] Total Materia, "Magnesium and Magnesium Alloys," January 2006. [Online]. Available: http://www.totalmateria.com/Article138.htm. [Accessed 25 January 2021].

[62] L. T. a. A. R. Austin Shaw, "Tensile Properties of High-purity Ca Metal," *British Journal of Applied Science & Technology*, vol. 15, no. 6, pp. 1-6, 2016.

[63] E. L. a. K. Abiko, "Tensile Properties of Commercially Pure, High-Purity and Ultra-High-Purity Iron: Results of an International Round-Robin," NIST Technical Note 1879, 2015.

[64] H. Li, "Corrigendum: Development of biodegradable Zn-1X binary alloys with," *Scientific Reports*, 2015.

[65] V. K. U. a. V. M. A, «Analysis of Mechanical Properties of Pure Aluminium Based Metal Matrix Composite,» *IJIRS*, vol. 3, núm. 5, 2014.

[66] R.P. Reed, Christopher N. Mccowan, Robert Wals, "Tensile strength and ductility of indium," *Materials Science and Engineering* , vol. 102, no. 2, pp. 227-236, 1988.

[67] MatWeb, "MatWeb Material property data," [Online]. Available: http://www.matweb.com/search/datasheet.aspx?matguid=64d7cf04332e428dbca9f755f4624a6c&ckck=1. [Accessed 27 January 2021].

[68] "EFFECT OF ANTIMONY ADDITION RELATIVE TO MICROSTRUCTURE AND MECHANICAL PROPERTIES OF CONTINUOUS CAST LEAD ALLOY," in *25th Anniversary International Conference on Metallurgy and Materials*, 2016.

[69] C. Smith, "Piezoresistance Effect in Germanium and Silicon," *Phys.Rev.*, vol. 94, no. 1, pp. 42-49, 1954.

[70] C. Euaruksakul, F. Chen, B. Tanto, C. S. Ritz, D. M. Paskiewicz, F. J. Himpsel, D. E. Savage, Zheng Liu., "Relationships between strain and band structure in Si(001) and Si(110) nanomembranes," *PHYSICAL REVIEW B*, vol. 80, no. 115323, 2009.

[71] A. D. a. A. U. S. Zh. Karazhanov, "Strain-induced modulation of band structure," *Journal of Applied Physics*, vol. 104, no. 024501, 2008.

[72] N. P. A. G. Y. N. K. Guilloy, «Germanium under high tensile stress: nonlinear dependence of direct band gap vs. strain,» *ACS Photonics*, 2016.

[73] Khaled S. Hameed and Adnan M. AL-Sheikh , "Theoretical Study of Energy Gap for Silicon and Germanium Under High Pressure," *Raf . Jou. Sci.*, vol. 22, no. 2, pp. 58-68, 2011.

[74] Jia Wang and Baojia Wu, "Pressure induced semiconductor–metal phase transition in GaAs: experimental and theoretical approaches," *RSC Advances*, vol. 12, 2016.

[75] K. H. A.-A. a. H. R. JAPPOR, "Electronic structure of Gallium Arsenide under pressure," *STRUCTURE OF THE MATTER*, no. 2, 2012.

[76] G. B. R. G. R. H. J. G. Leila Balaghi, «Widely tunable GaAs bandgap via strain engineering in core/shell nanowires with large lattice mismatch,» *Nature Communications*, núm. 10, p. 2793, 2019.

[77] B. W. J. W. H. Z. H. L. Guozhao Zhang, «Metallization and Electrical Transport Behaviors of GaSb under High-Pressure,» *Scientific reports*, vol. 7, núm. 2656 , 2017.

[78] AZO Materials, "A Background to Silicon and its Applications," 20 July 2001. [Online]. Available: https://www.azom.com/properties.aspx?ArticleID=599. [Accessed 12 January 2021].